

## **NASA Contractor Report 172479**

NASA-CR-172479  
19850007170

# **Advanced Infrared Laser Modulator Development**

**P.K. Cheo, R. Wagner, M. Gilden**

**UNITED TECHNOLOGIES RESEARCH CENTER  
EAST HARTFORD, CT 06108**

**Contract NAS1-16904  
December 1984**

**LIBRARY COPY**

JAN 24 1985

**LANGLEY RESEARCH CENTER  
LIBRARY, NASA  
HAMPTON, VIRGINIA**



National Aeronautics and  
Space Administration

**Langley Research Center**  
Hampton, Virginia 23665



1. The first part of the document is a letter from the President of the United States to the Congress, dated January 1, 1801.

2. The second part is a report from the Secretary of the Treasury, dated February 1, 1801.

3. The third part is a report from the Secretary of the Navy, dated March 1, 1801.

4. The fourth part is a report from the Secretary of the War, dated April 1, 1801.

5. The fifth part is a report from the Secretary of the Interior, dated May 1, 1801.

## Advanced Infrared Laser Modulator Development

### TABLE OF CONTENTS

	<u>Page</u>
1.0 TECHNICAL REPORT SUMMARY . . . . .	1-1
1.1 Project Objectives . . . . .	1-1
1.2 Project Goal . . . . .	1-1
1.3 Summary . . . . .	1-2
2.0 INTRODUCTION . . . . .	2-1
3.0 SYSTEM DESCRIPTION . . . . .	3-1
4.0 ELECTROOPTIC INFRARED WAVEGUIDES . . . . .	4-1
5.0 INTEGRATION OF MICROWAVE CIRCUITRY . . . . .	5-1
6.0 FABRICATION TECHNIQUES . . . . .	6-1
7.0 RESULTS AND DISCUSSION . . . . .	7-1
8.0 REFERENCES . . . . .	8-1

N85-15479#



## 1.0 TECHNICAL REPORT SUMMARY

### 1.1 Project Objectives

A need exists for a high resolution and continuous tuning of a coherent infrared laser source in the wavelength range from 9 to 12 microns. This research and development project is directed toward the establishment of a reproducible and reliable device that utilizes an integrated optical approach to generate tunable optical sidebands by electrooptic modulation of an infrared laser source at microwave frequencies. The objective of the first phase of this project is to demonstrate the reproducibility of microwave characteristics of a unique E-O modulator in a non-conventional configuration. Because of its physical dimensions, a number of problems related to the device impedance, effective dielectric constants, and very large scale geometric perturbations must be determined and properly addressed. The objective of the second phase of this project is to investigate the overall device characteristics in terms of its electrooptic properties, such as optical transmission, modulation efficiency, frequency tuning range and far-field beam profile.

### 1.2 Project Goal

The goal of this project is to produce an efficient, wide bandwidth infrared modulator, which shall provide the following minimum performance characteristics:

- A modulation bandwidth  $> 10$  GHz (3 dB)
- Optical transmission  $> 30\%$  at  $\lambda = 10.6 \mu\text{m}$ .

### 1.3 Summary

United Technologies Research Center has developed the necessary technologies and has fabricated, tested and delivered an advanced infrared laser modulator to NASA-Langley. The performance characteristics of the above mentioned device have exceeded the goal of the project as stated in 1.2.

This technical report provides a tutorial review of the microwave-tuned IR waveguide modulator, which is used to generate a continuously tunable and frequency-synthesized sideband power in 9 to 11  $\mu\text{m}$ . Details are given on the system configuration, design parameters, trade-off analysis, system optimization, and fabrication procedures, along with measured performance characteristics.

## 2.0 INTRODUCTION

Continuous tuning of a  $\text{CO}_2$  laser by phase modulation at microwave frequencies in GaAs thin film waveguides has been reported (Refs. 1 and 2) previously. In optical waveguides, extremely intense optical and microwave fields can be established, provided that special techniques are used to couple optical and microwaves efficiently into the device. If these two waves are properly synchronized with nearly the same phase velocity, very efficient and broadband modulation can be achieved. Phase modulation of  $\text{CO}_2$  lasers at microwave frequencies with linear polarization will generate both the upper and the lower sideband frequencies, which can be well resolved from the laser carrier frequency  $f_0$ . By varying the microwave frequency  $f_m$ , it is possible to tune the sideband power over a certain range. The tuning range depends critically on the modulator structure. One of the difficulties in previous work has been in obtaining very broadband and uniform frequency response. Another difficulty from earlier work is that the device has an excessive loss, which is caused primarily by the absorption of the microstrip electrode and the metallic ground plane.

In this study, efforts have been made to avoid these problems by integrating into two types of waveguide structures with two microwave impedance matching circuits, which consist of three  $\lambda/4$  step transformers. One of the two waveguides is made of a thin GaAs slab with an ion-beam milled channel, and the other one is also made of GaAs in the form of a multilayered structure. A traveling-wave microstrip transmission line is fabricated in these waveguides to form the state-of-the-art integrated optical modulators. These modulators are used to generate sidebands from a line-selectable  $\text{CO}_2$  laser by phase modulation of an

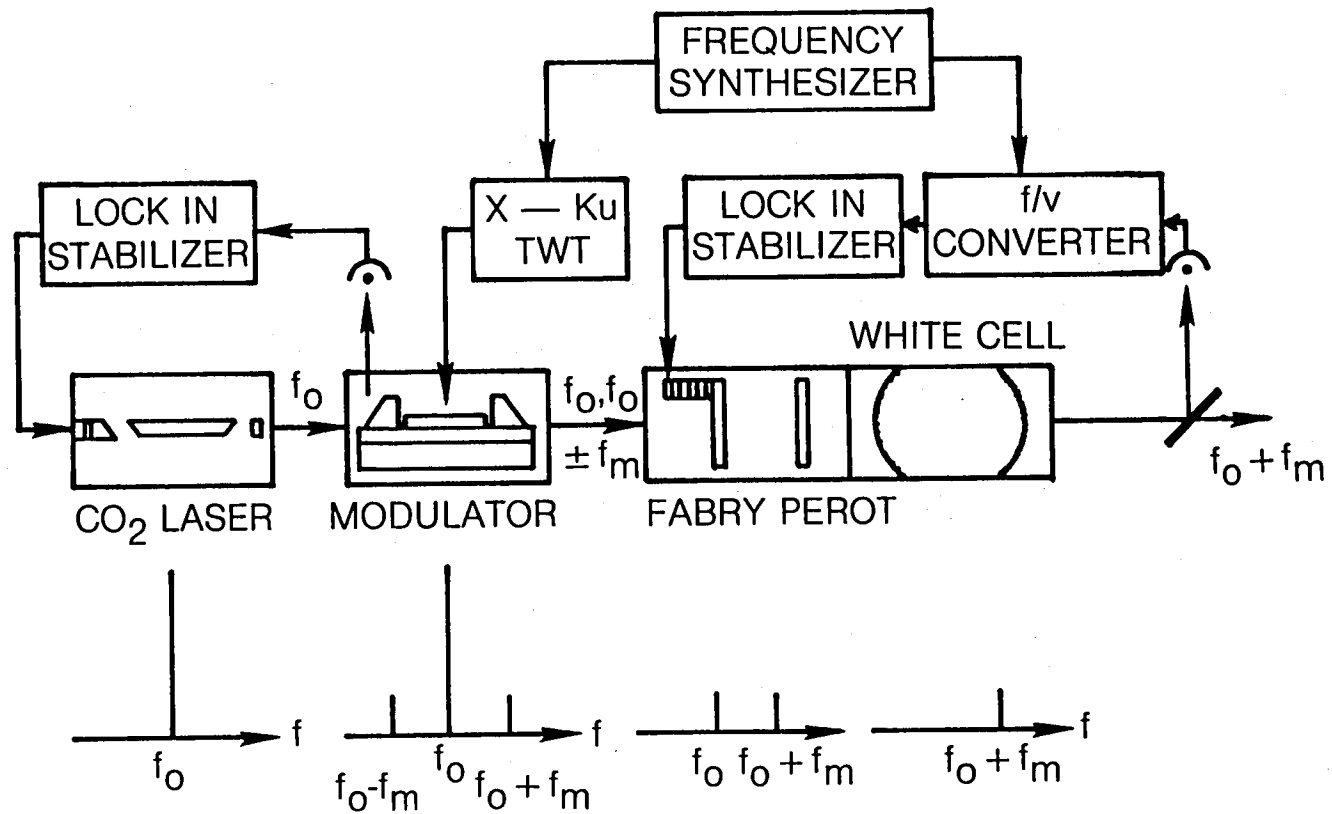
optical guided-wave in the GaAs active layer at microwave frequencies. A total of 30 GHz frequency tuning range in two sidebands at power levels above 100 mW has been obtained with these devices. This paper will first describe the overall system and its performance characteristics. It is followed by a brief description of the waveguide structures and a detailed discussion of the techniques for integrating the microwave circuitry into an optical waveguide. An optimum configuration has been established by a trade-off analysis involving a number of parameters. A procedure for fabricating waveguide modulators is presented which involves primarily hybrid microelectronics technology, and provides very reliable and reproducible results. This tunable IR source is developed primarily for the purpose of remote sensing of the atmosphere (Ref. 3), but it can also be used as a convenient and reliable analytic tool for very high resolution spectroscopic studies or for other applications such as isotope separation and frequency multiplex communication.



### 3.0 SYSTEM DESCRIPTION

Figure 1 is a block diagram of the system. It consists of five components. The first one is a single frequency, line selectable and actively stabilized  $\text{CO}_2$  laser with a Gaussian beam of a spot size  $\omega_0$  (full width at half maximum FWHM) of about 1 mm. The second one, which is the most essential system component, is a GaAs thin film waveguide modulator integrated with a microwave transmission line. The microwave is provided by amplifying a low power signal from a frequency synthesizer through a high power and broadband traveling-wave tube (TWT) amplifier operating in the X and Ku bands. The third one is a Fabry-Perot (FP) interferometer having a finesse of about 30. The fourth one, which is not absolutely necessary for many applications, is a White cell filled with heated  $\text{CO}_2$  gas, and the last one is an IR photodetector and a storage scope. The  $\text{CO}_2$  laser beam is allowed to expand to a size  $\omega_0$  of about 8 mm and is then focussed to about 0.3 mm by a mirror. This focussed spot is directed at the front surface of a germanium right angle prism, which is oriented at an angle phase-matched to the transverse electric ( $\text{TE}_1$ ) mode of the waveguide. The Ge prism is in pressure-contact with the waveguide surface, and can transfer about 80 percent of the input laser power from a Gaussian beam in the air into a waveguide mode through the evanescent-wave gap-spacing. As the  $\text{TE}_1$  mode propagates along the entire length ( $\sim 3.5$  cm) of the guide, its power is attenuated to a certain extent by the two electrodes. The total optical power  $P_T$  transmitted through the waveguide after accounting for the electrodes' attenuation and coupling losses of two Ge prisms, varies from 25 to 36 percent of the input power  $P_0$ . This value depends critically on the quality of the guide, and can be increased

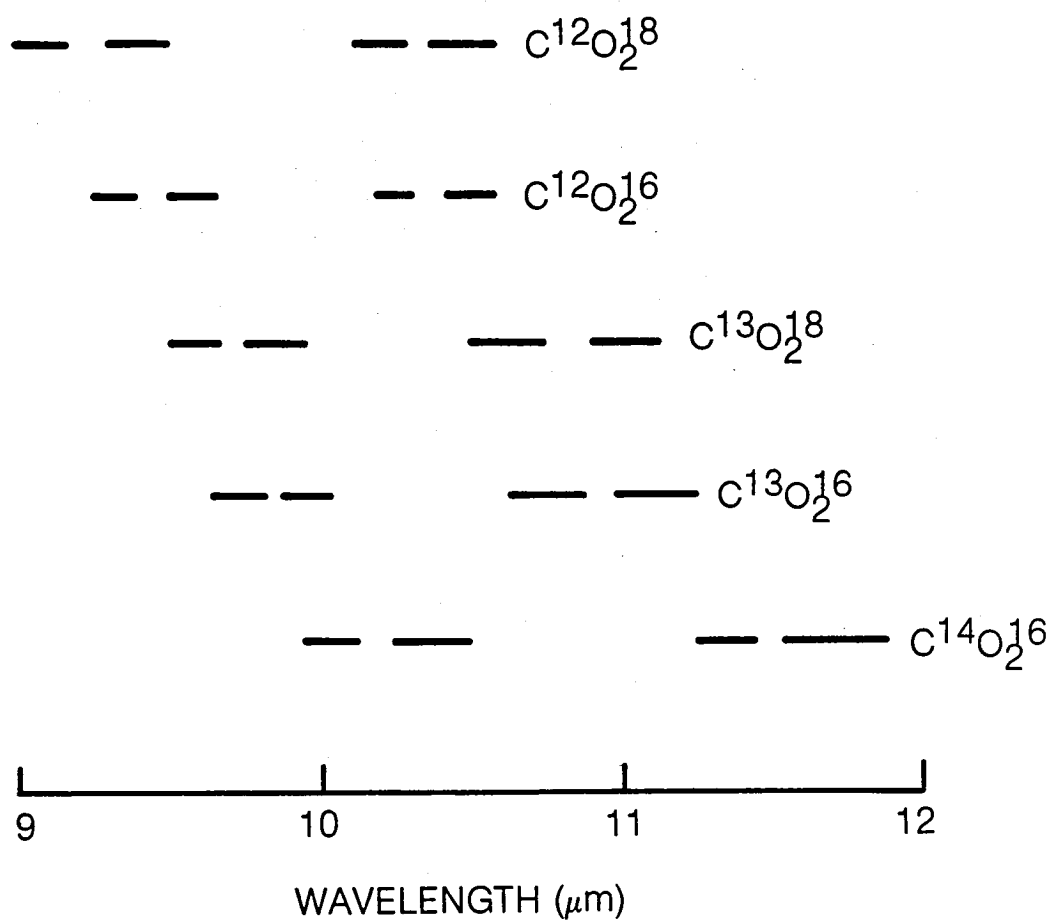
FIG. 1 SYSTEM BLOCK DIAGRAM OF A TUNABLE IR LASER SOURCE



significantly by using a multilayered modulator structure to be discussed in the next section. When microwave power is applied to the modulator, the spectral output splits into three distinct frequencies,  $f_o$  and  $f_o \pm f_m$ , each of which can be preferentially selected by a tunable FP filter. The former  $f_o$  is the laser carrier frequency and the latter  $f_o \pm f_m$  are the frequencies of the sidebands. Because of very large carrier power  $P_T$ , the FP filter usually is inadequate to eliminate the carrier power completely. Typical sideband to carrier power ratio is of the order of unity, when the filter is tuned to the peak of the sideband. If the modulated output passes through both the FP filter and a White cell, the carrier power can be eliminated almost completely.

Spectroscopy of the vibrational-rotational lines of  $CO_2$  lasers in the 9 to 11  $\mu m$  region has been studied in great detail (Ref. 4). The separation between these laser transitions is about 60 GHz. With the above technique, tunable sideband power can be generated to cover almost 1/2 of the spectral spacing separated between two laser lines. For complete spectral coverage in the 9 to 12  $\mu m$  range, it is necessary to use several isotopic  $CO_2$  lasers. Figure 2 shows the emission regions of five isotopic  $CO_2$  lasers (Ref. 5). Using two different  $CO_2$  lasers, i.e.,  $C^{12}O_2^{16}$  and  $C^{13}O_2^{16}$ , it is possible to tune over almost the entire spectral range from 9.2 to 11.2  $\mu m$ . With a programmable frequency synthesizer (HP Model 8672A), one can achieve frequency accuracy to within one Hz. The fundamental limitation of this technique is the frequency stability of the laser. Short-term frequency stability of typical low power  $CO_2$  lasers constructed with super-invar materials can be kept to within 10 kHz. The long-term stability can easily be maintained to within 100 kHz with the help of a lock-in stabilizer. By using

FIG. 2 FIVE ISOTOPIC CO<sub>2</sub> LASER TRANSITION BANDS



a 20 W laser and 30 W for the microwave as the input, the output power over 100 mW in a single sideband can be obtained from a simple channeled GaAs waveguide modulator without buffer layers. The sideband power can be increased by about a factor of two if two ZnSe buffer layers of about 1 to 2 microns in thickness are deposited on the surfaces of the GaAs thin-film so that the energy of the guided-wave is confined almost completely within the dielectric materials.

The entire system can be packaged into a volume roughly 2'x3'x4' as shown in Fig. 3. Figure 3 shows only the optical components which include a RF excited CO<sub>2</sub> waveguide laser, a microwave tuned IR waveguide modulator, a White cell, a FP filter and a HgCdTe photodetector. The microwave components (not shown in this figure) are mounted underneath the honeycomb plate. The laser line is selected by adjusting the angle of the diffraction grating mirror, which can be controlled by using a stepping motor-driven mechanism. For each vibrational-rotational laser line, a spectral range of 30 GHz frequency synthesized outputs, as shown in Fig. 4, can be either automatically tuned over the two sidebands by sweeping over the entire range from 5 to 20 GHz or selectively locked onto any frequency of interest. In either case, a reference signal  $f_m$  from the microwave oscillator is needed to set the FP-PZT voltage  $V$  with the help of a  $f_m/V$  transfer function, calibrated to the peak transmission of the sideband power. This tunable IR laser source provides extremely reliable service, which has been established by the actual performance of these devices. One of the earlier waveguide modulators is still in good operating condition after service a period of eight years. Of most importance, are the convenience and maintenance free operation, primarily because the system operates at room temperature as compared to other IR tunable

FIG. 3 A LABORATORY MODEL OF A MICROWAVE-TUNED CO<sub>2</sub> LASER

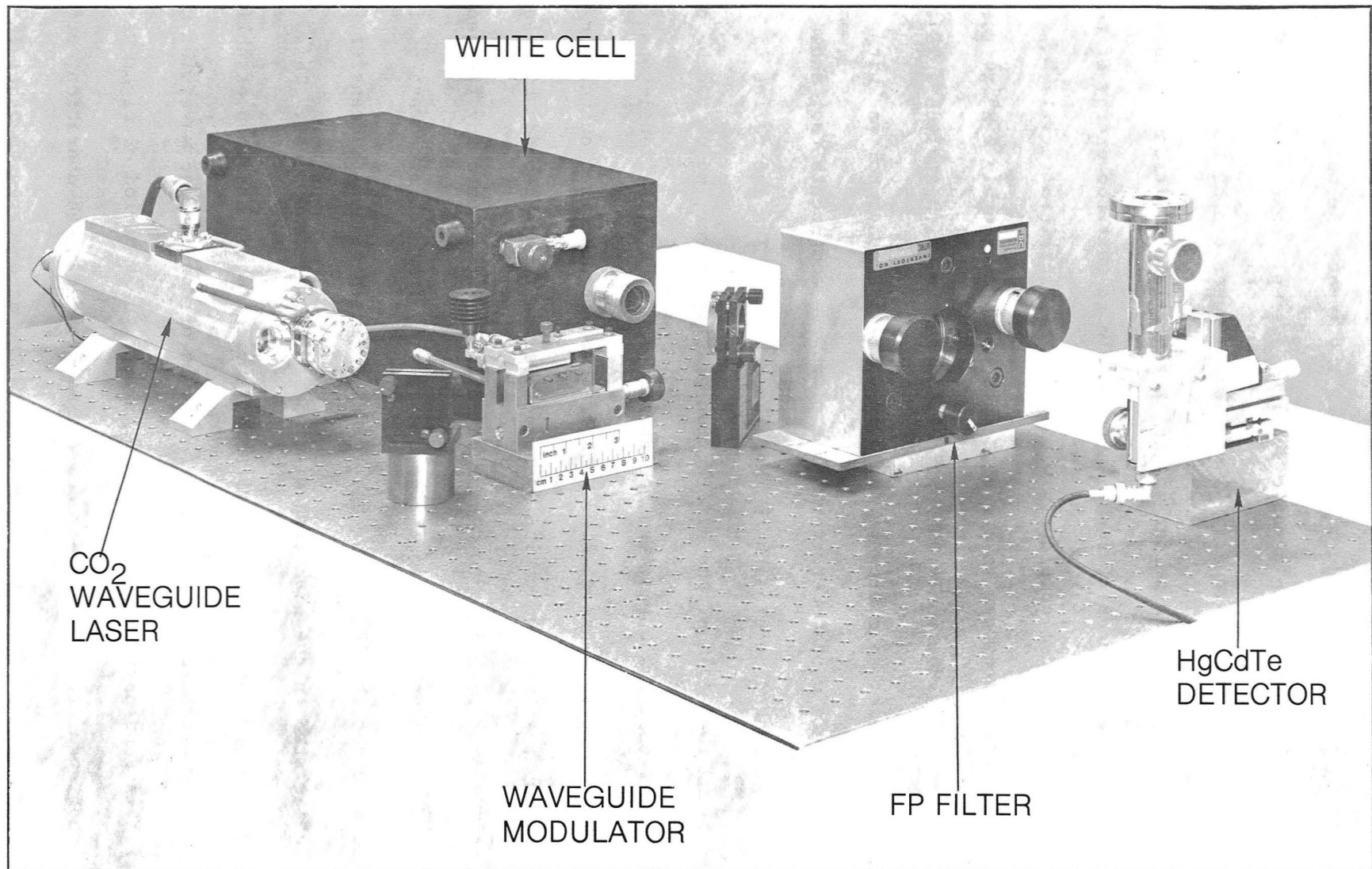
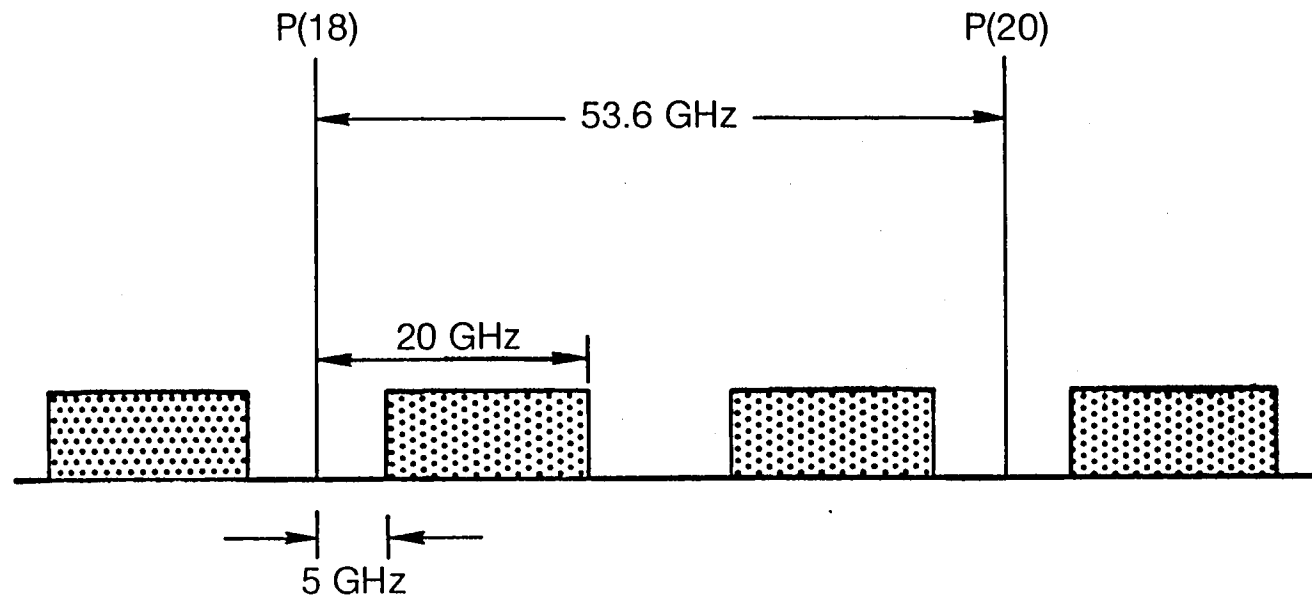


FIG. 4 SPECTRAL CHARACTERISTICS OF A TUNABLE CO<sub>2</sub> LASER



sources such as lead-salt diode lasers (Ref. 6), all of which require cryogenic cooling. With frequency synthesized outputs, the system provides the highest degree of frequency accuracy without the need of a spectrometer, as required by all lead-salt laser diodes. In terms of output power, this system can deliver more than 100 times the output of typical lead-salt diode lasers.

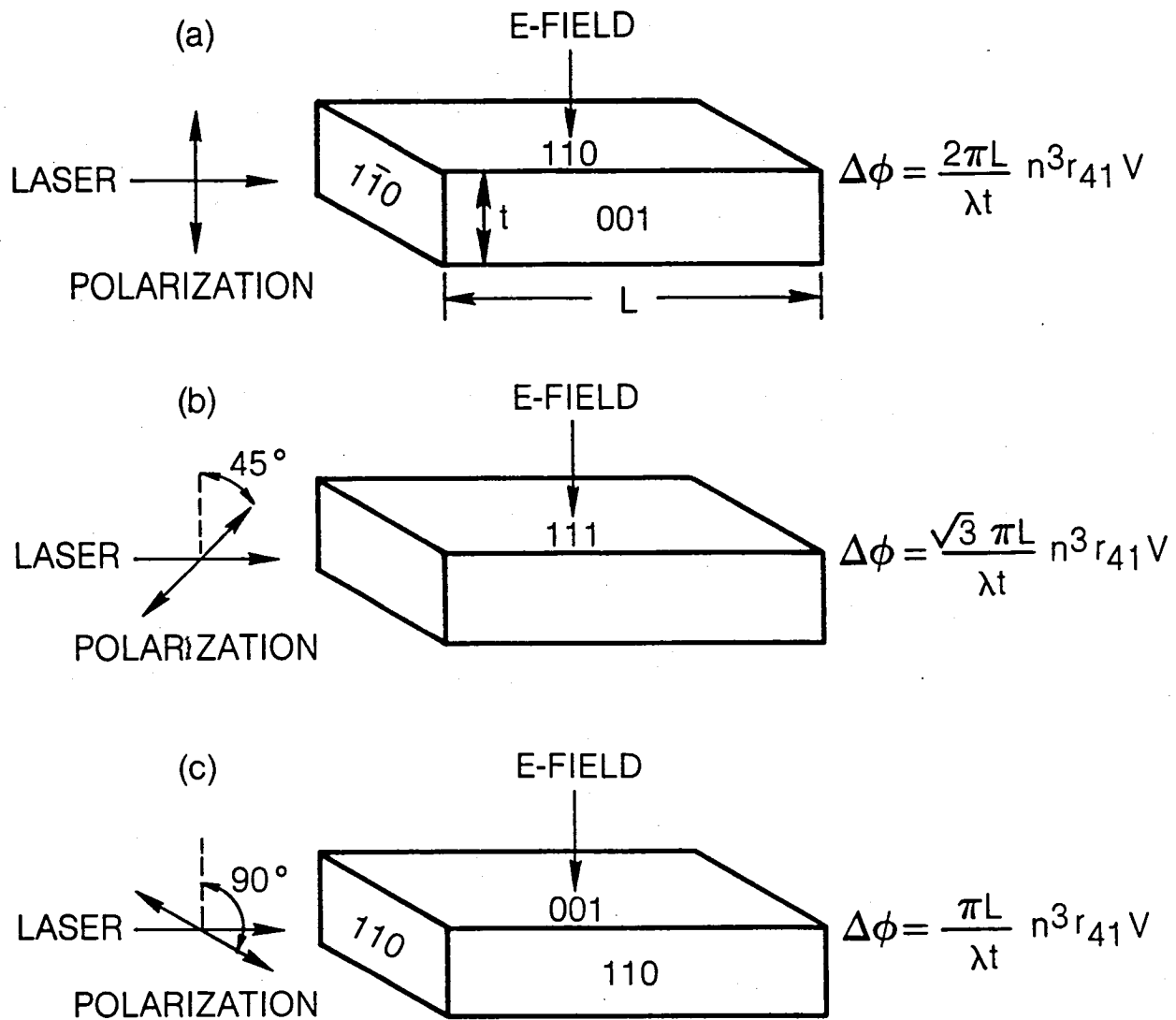


#### 4.0 ELECTROOPTIC INFRARED WAVEGUIDES

The most unique feature of the system is the use of an electrooptic waveguide without which it is impossible to generate sidebands over such a wide tunable range. Even at a very narrow bandwidth (0.5 GHz), bulk modulators (Ref. 7) require many kilovolts as compared with only a few volts to produce an equivalent modulation depth by using a waveguide modulator. CdTe and GaAs are the two infrared electrooptic materials commonly used to make bulk modulators. To fabricate thin-film waveguides at a thickness of 25  $\mu\text{m}$ , material must be free from defects. It has been difficult to obtain defect-free CdTe of large size. On the other hand, large areas (3"x3") GaAs wafers with excellent quality can be purchased at very reasonable cost. For this reason, techniques for processing thin-film waveguide material have been developed exclusively for GaAs, even though CdTe can, in principle, offer a factor of two to four over-all modulation efficiency over than obtainable from GaAs, if large crystal of good quality becomes available. When this occurs, techniques have to be modified to process CdTe material and re-design the microwave circuitry in accordance with its properties.

There are several crystal orientations from which one can obtain phase modulation. Figure 5 shows three different cuts of the GaAs crystal, the directions of laser polarization, the electric field, and the propagation of optical wave. Because of the difference in induced birefringence along various crystal axes, the depth of modulation at a given E-field amplitude will vary with varying

FIG. 5 PHASE MODULATION OF A POLARIZED LASER BEAM  
USING GaAs ELECTRO-OPTIC CRYSTALS



orientation. The particular orientation shown in Fig. 5(C) is chosen in this work because it is a preferential one for chemo-mechanical polishing and low propagation losses associated with guided-wave modes. More details on waveguide fabrication will be presented later. For a guided-wave (TE modes) propagating in the (110) direction with a polarization parallel to the plane of the guide, the change of refractive index  $\Delta n$ , when a dc voltage  $V$  is applied in the direction of (001), is given by

$$\Delta n = \frac{1}{2t} n^3 r_{41} V \quad (1)$$

where  $t$  and  $r_{41}$  are the thickness and the electrooptic coefficient of the guide. The corresponding change in phase  $\phi$  of the light as it travels through a distance  $L$  is given by

$$\Delta\phi = kL\Delta n = \frac{\pi L}{\lambda t} n^3 r_{41} V \quad (2)$$

If the field is a traveling microwave, oscillating at a frequency  $f_m$ , the expression for  $\Delta\phi$  given in Eq. (2) must be corrected by taking into account the difference in velocities between the guided optical wave and the microwave. The correction factor  $C$  is given by

$$\Delta\phi = C kL\Delta n \quad (3)$$

where

$$C = \operatorname{Re} \int_0^L \exp [-\alpha x + i\Delta\beta(x - L/2)dx] \quad (4)$$

In Eq. (4),  $\text{Re}$  represents the real part of the integral in which the first term represents the absorption loss of microwave and the second term is also a loss term resulting from the difference  $\Delta\beta$  in propagation constants. It is important to design a structure such that two waves are synchronized. Measurements on microwave properties of GaAs and methods for synchronization and impedance matching will be presented in the following section.

Because the phase of the guided wave is modulated at  $f_m$ , the amplitude of the spectral output can be expressed by a power series in terms of Bessel function  $J_n$  as follows:

$$E = E_0 J_0(\Delta\phi) \sin(2\pi f_0 t + \phi_0) + \sum_{n=1}^{\infty} E_0 \left\{ J_n(\Delta\phi) \sin(2\pi f_0 t + 2\pi f_m t + \phi_0) - J_n(\Delta\phi) \sin(2\pi f_0 t - 2\pi f_m t + \phi_0) \right\} \quad (5)$$

where the first term is the carrier field which is unmodulated. The second term associates with various orders of sidebands. The first term in the bracket goes with the upper and the second goes with the lower sidebands. Since  $\Delta\phi$  is usually very small, only the first order of Bessel functions,  $J_1$ , in the series is retained and the expressions for  $J_0$  and  $J_1$  can be approximated by 1 and  $\Delta\phi/2$ . Therefore, the ratio of the sideband to the carrier power can be expressed as

$$P_s/P_0 = 2J_1^2 = \Delta\phi^2/2 \quad (6)$$

Two different waveguide structures have been used in this work. The topology of the first one is a simple channelled 3-D waveguide SCWG having a thickness of 25  $\mu\text{m}$ . This structure has been described in detail previously

(Ref. 8). In this work, further improvement has been made by integrating a three  $\lambda/4$  impedance matching network into the structure. The second one is a multi-layered structure MLWG, which has been investigated for the purpose of reducing optical losses. The SCWG can be routinely fabricated and yields consistent performance. The disadvantage of this structure is the excessive loss, which limits the optical transmission to about 25 to 36 percent. For the purpose of comparing the performance of the two types of waveguides, some of the useful results for the TE modes are summarized here only for the TE modes.

The field relations in a planar waveguide with its thickness oriented in the x-direction and the propagating vector  $\bar{k}$  as shown in Fig. 6 are:

$$\beta E_y = -\mu\omega H_x \quad (7)$$

$$i\partial H_x + \frac{\partial H_z}{\partial x} = -i\epsilon\omega E_y \quad (8)$$

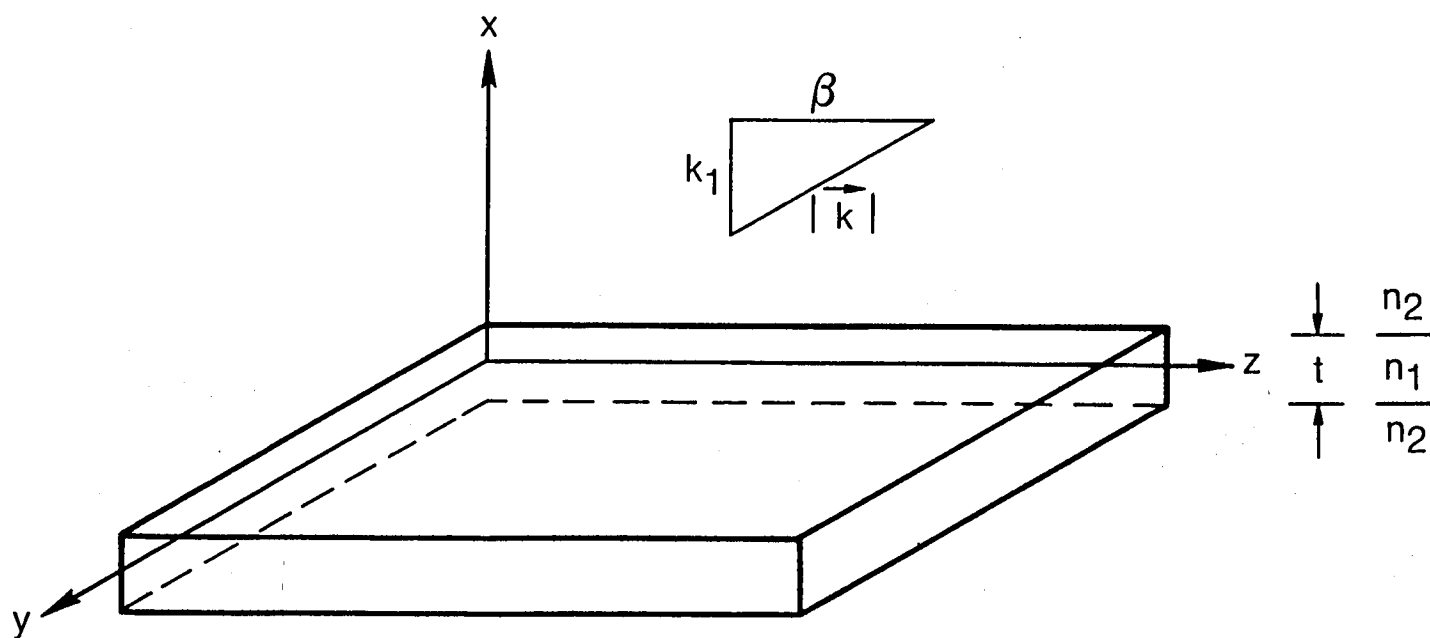
$$\frac{\partial E_y}{\partial x} = i\epsilon\omega H_z \quad (9)$$

All other components vanish because  $\partial/\partial y=0$ . We shall assume  $E_y$  of a simple form:

$$E_y \propto \exp ik_1 x \quad |x| \leq t/2 \quad (10)$$

Where  $|x| > t/2$ , the fields must be modified by introducing an evanescent decay tail as given by the expression:

FIG. 6 THE COORDINATE SYSTEM FOR A PLANAR WAVEGUIDE



$$E_y \propto \begin{cases} \cos(k_1 t/2) \exp -\gamma_2(|x| - t/2) & \text{even order} \\ x \sin(k_1 t/2) \exp -\gamma_2(|x| - t/2) & \text{odd order} \end{cases} \quad (11)$$

where  $k_1$  is the x-component of  $\vec{k}$  in medium 1, and  $\gamma_2$  is the decay constant of the evanescent waves in medium 2. The eigenvalue equation for the TE modes can be obtained by imposing the boundary conditions that the sum of the phase change upon total reflection from the upper and lower guiding layers must be an integer multiple of  $2\pi$ . This leads to the following equation:

$$k_1 = \frac{1}{t} (2 \tan^{-1} \frac{\gamma_2}{k_1} - 2 m\pi) \quad (12)$$

where  $m=0,1,\dots$ , representing the orders for the TE modes.  $k_1$  is related to the propagation constant  $\beta$  of various guided-wave modes by the relation

$$k_1^2 = n_1^2 k_0^2 - \beta^2 \quad (13)$$

where  $k_0 = 2\pi/\lambda$ , the propagation constant in free space.

Figure 7 shows plots of  $\beta/k_0$  as a function of waveguide thickness for three different structures. The indices for these structures are:  $n_1 = 3.3$  for the guiding layer,  $n_2 = 1.0$  for the surrounding media without buffer layers, and  $n_2 = 2.6$  for the surrounding media with buffer layers (Ref. 9). Figure 8 shows the calculated values of the absorption coefficient in dB/cm as a function of waveguide thickness having the electrodes lying on both the top and the bottom of these guides to form a complete modulator structure.

FIG. 7 CALCULATED  $\beta/k_0$  VALUES VS THE WAVEGUIDE THICKNESS

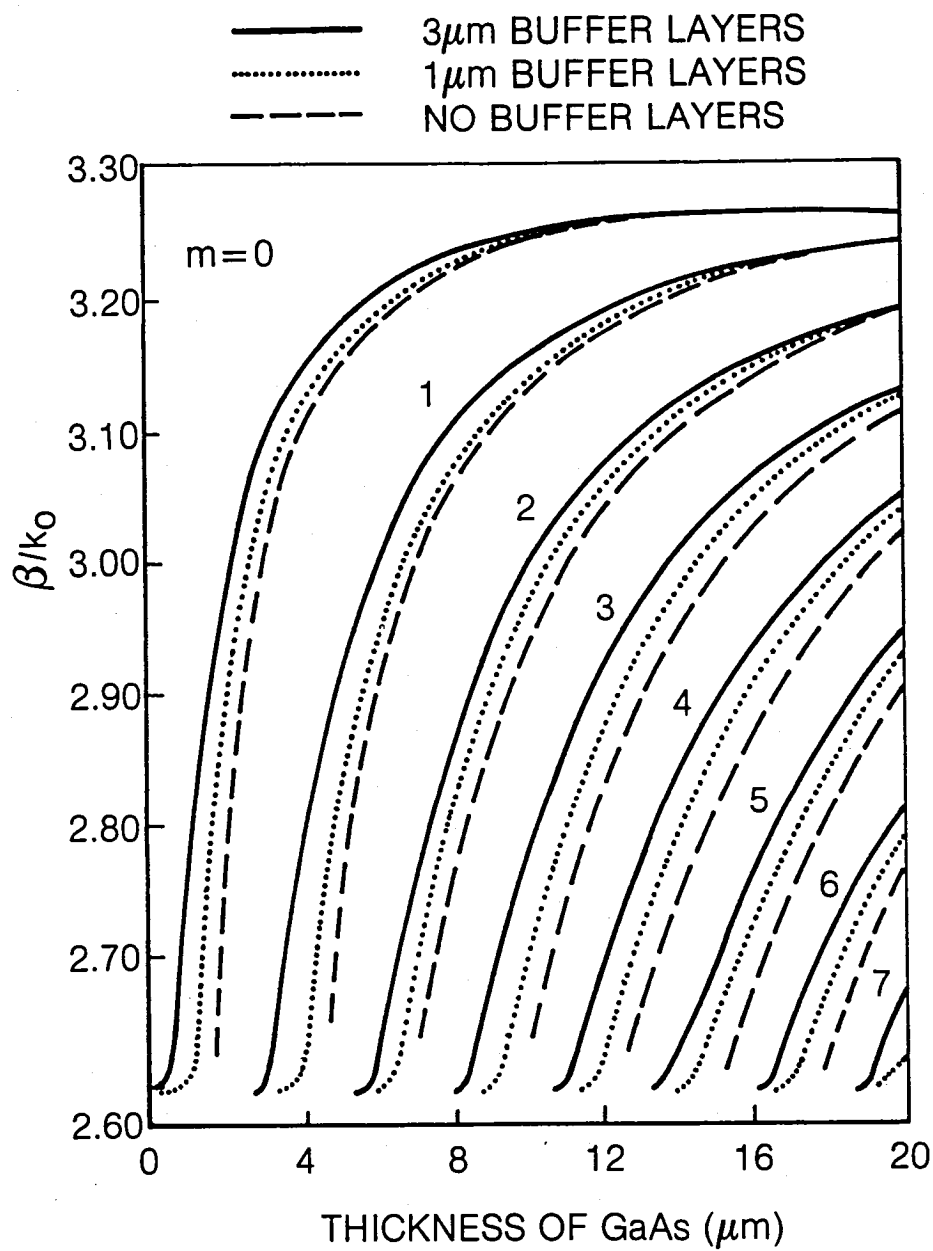
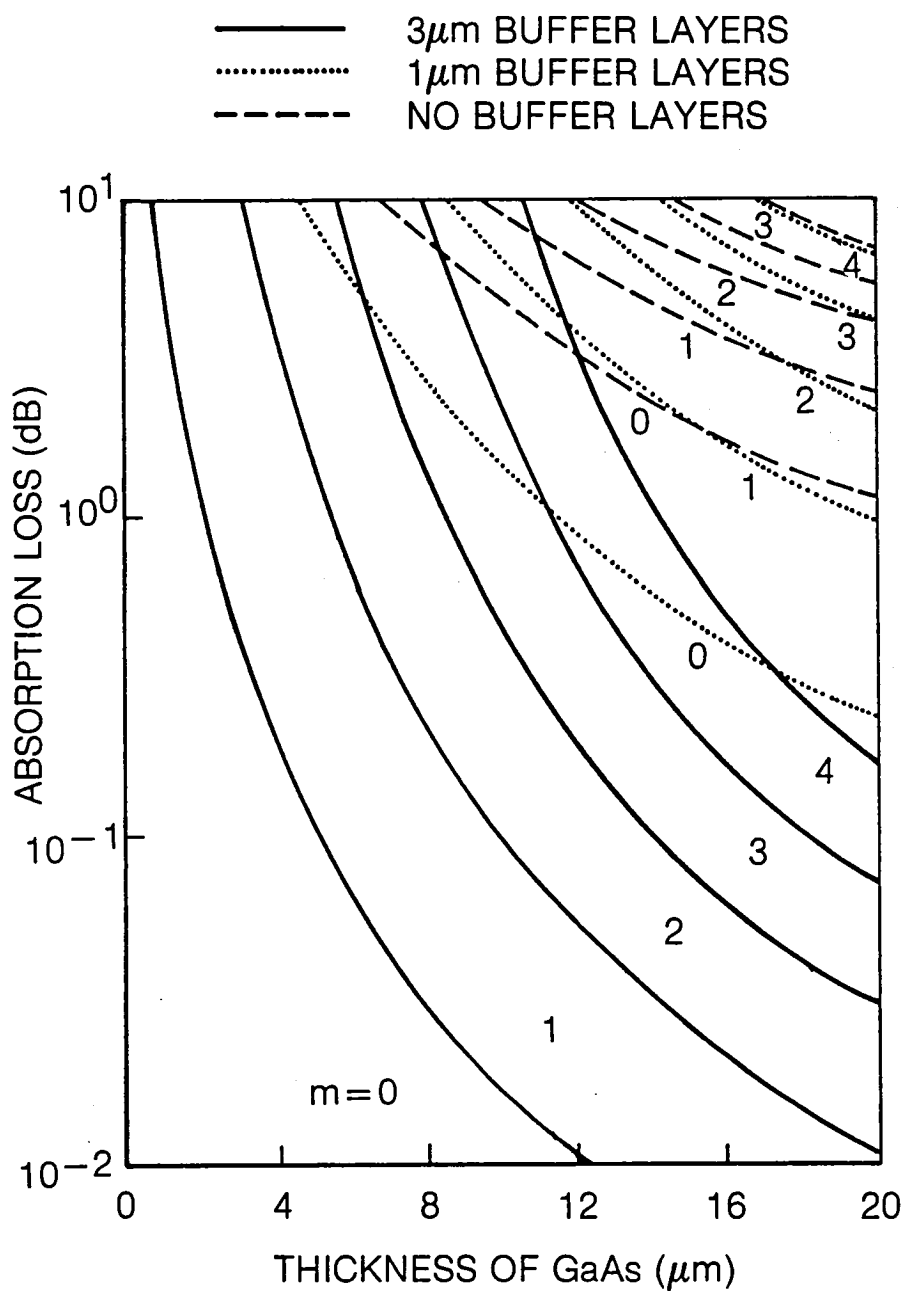




FIG. 8 ABSORPTION LOSS IN dB FOR THE TE MODES



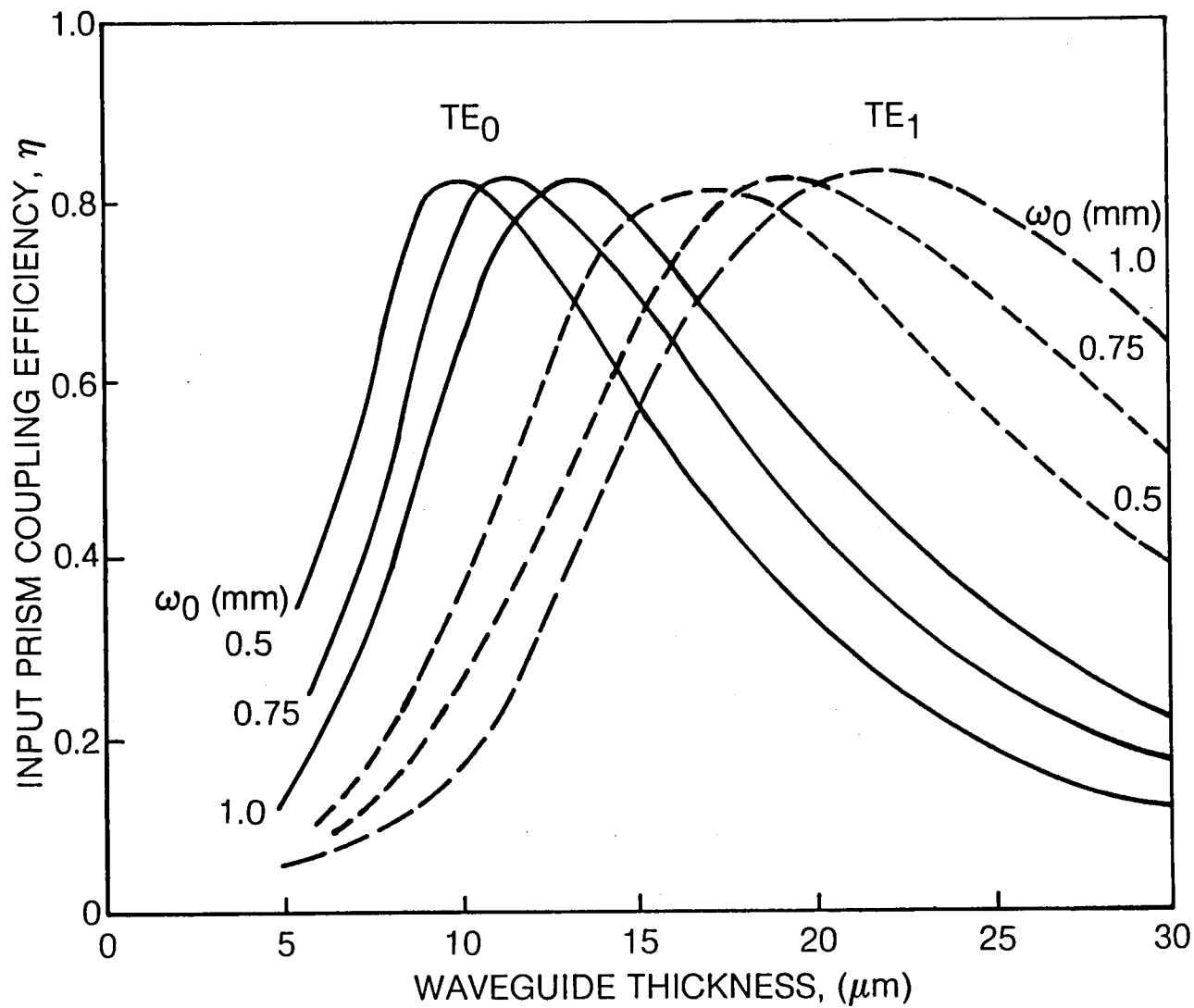
To establish a guided-wave mode in a waveguide, the most efficient method is to use a prism coupler (Ref. 10). Optical coupling between a Gaussian beam of a spot size  $\omega_0$  (HWFH) and a guided-wave mode through the evanescent wave coupler depends critically on both phase and aperture matching. Assuming that a perfect phase matching is established by adjusting the angle of incidence, the relationship between the coupling efficiency  $\eta$  and the aperture, which is usually determined by the beam size, is given by

$$\eta = \frac{1}{\alpha \omega_0} [1 - \exp(-2\alpha \omega_0)]^2 \quad (14)$$

where  $\alpha$  is the coupling parameter and is a complicated function of waveguide thickness, refractive index, gap spacing  $\delta$  between the prism base and the surface of the guide. Figure 9 shows the calculated results of  $\eta$  as a function of  $t$  for three different values of  $\omega_0$  and for  $TE_0$  and  $TE_1$  modes by keeping  $\delta = 0.1 \mu\text{m}$ . The  $\eta$  values vary only slightly with  $\delta$  values for  $\delta < 0.1 \mu\text{m}$ . In practice, it is very easy to obtain a gap-spacing to within  $0.1 \mu\text{m}$  by using a pressure-contact. This is not true for laser systems at shorter wavelengths. To obtain a broad modulation bandwidth, it is desirable (see next section) to use a narrow electrode, however, this puts a restriction on the size of the laser beam, and can affect the over-all efficiency of the modulator.

For a 1 mm wide WG channel, the optimum optical coupling for the  $TE_0$  mode can be obtained at a thickness of  $15 \mu\text{m}$ . On the other hand, the propagation loss becomes too excessive in a  $15 \mu\text{m}$  thick guide without buffer layers because of the electrode absorption. As the thickness increases, the propagation loss decreases

FIG. 9 PRISM COUPLING EFFICIENCY FOR TE MODES  
(GAP-SPACING=0.1  $\mu\text{m}$ )



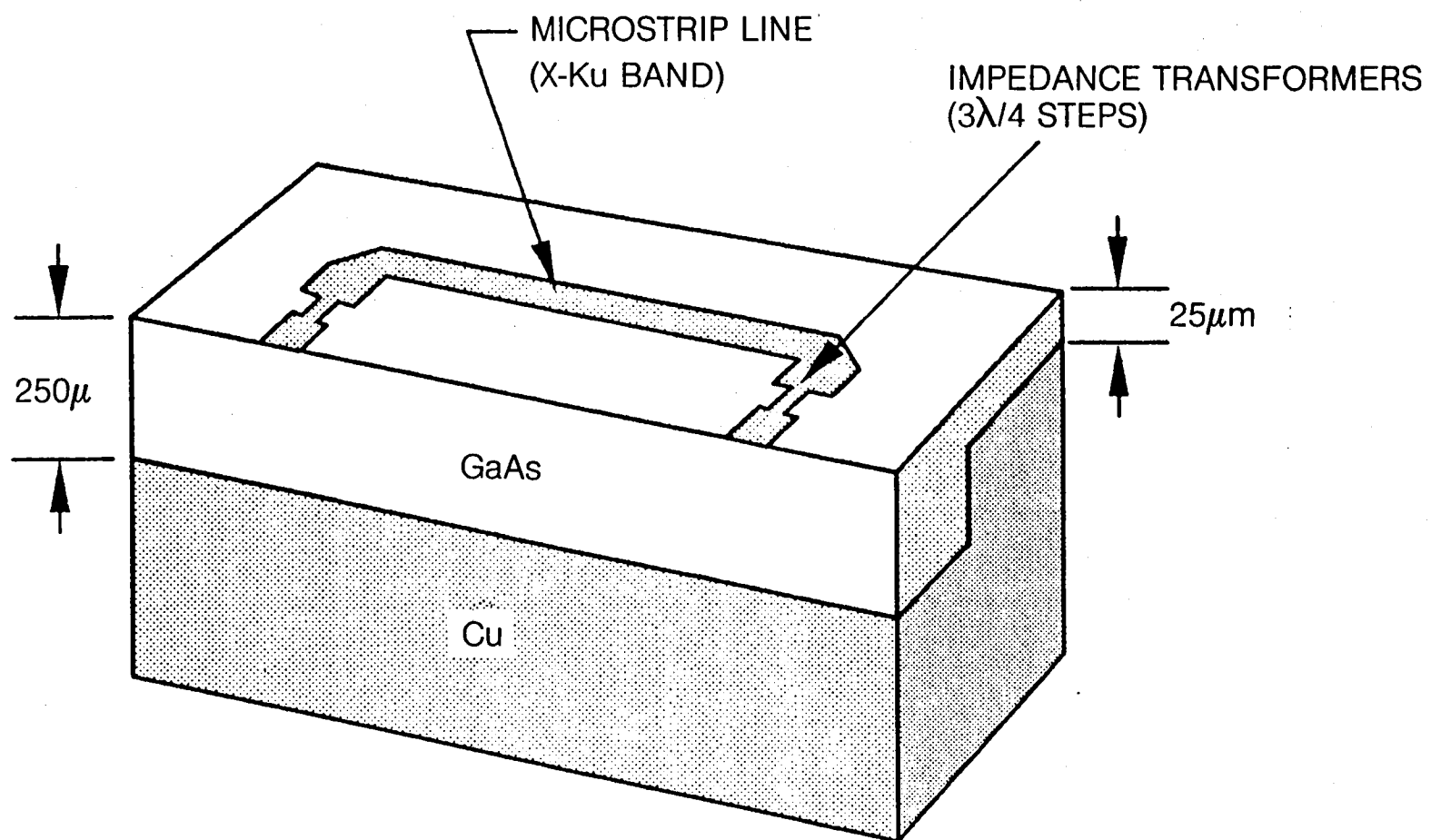
rapidly. A tradeoff between the coupling and propagation losses had led to the choice of 25  $\mu\text{m}$  for waveguide thickness. At 25  $\mu\text{m}$ , the optimum coupling of 1 mm spot size is for the  $\text{TE}_1$  mode. Because of the difference in their field distribution in the guide, the  $\text{TE}_1$  mode usually has a higher propagation loss than the  $\text{TE}_0$  mode. However, the total loss for a  $\text{TE}_1$  mode in a 25  $\mu\text{m}$  guide is less than that for a  $\text{TE}_0$  mode in a 15  $\mu\text{m}$  guide. There are other ways to reduce the losses, for example, by using a tapered raised-ridge waveguide (Ref. 8), but fabrication of such a structure is very difficult and has not been very reliable. Another way to reduce the propagation loss is to employ a multi-layered waveguide. The topology of such a guide consists of a guiding layer of a 15  $\mu\text{m}$  GaAs thin film, over which a thin (1-3  $\mu\text{m}$ ) ZnSe layer is deposited on both surfaces by ion-beam sputtering. These layers provide a buffer zone between the waveguide and the electrode. With this structure, optical transmission can be increased by about 50 percent from the result obtained with a simple channeled waveguide having an identical propagation length.

## 5.0 INTEGRATION OF MICROWAVE CIRCUITRY

To make a microwave tuned waveguide modulator, it is necessary to fabricate an appropriate electrode on the thin slab of GaAs with a metallic ground plane on one of the two surfaces. The electrode must be properly designed by synchronizing the guided IR wave with the traveling microwave in order to achieve highest modulation efficiency. From a microwave standpoint, an optimum electrode configuration, as shown in Fig. 10, is a microstrip transmission line with a good impedance matching to the source and the termination so that a very broad modulation bandwidth can be achieved. Other structural configurations such as slotlines, and dielectrically filled ridge waveguides have also been investigated (Ref. 11) and found to be very difficult to reproduce. The major difficulty is due to the extremely close tolerance required for constructing these devices. Microstrip structure turns out to be the most reliable one, because it can be fabricated by using a photolithographic technique to the desired accuracy. The optimum modulator cross-section can be derived from a simple model with the assumption that a uniform distribution of the microwave field  $E_m$  exists in the active region. The microwave power in the same region can be expressed by

$$P_m = \frac{E_m^2}{Z_0} tW \sqrt{\epsilon_1} \quad (15)$$

FIG. 10 TOPOLOGY OF A TRAVELING-WAVE IR WAVEGUIDE MODULATOR



where  $Z_0$  is the plane-wave characteristic impedance of free space,  $E_m$  is the field amplitude of the microwave,  $t$  is the thickness and  $W$  is the width of the active region. To minimize the power requirement, the dimensions of the active region must be chosen as small as possible. As a result, the value of the characteristic impedance becomes relatively low, therefore, proper impedance transformers must be designed to provide a broadband matching. As indicated in the previous section, the optimum coupling length for the  $TE_1$  mode in the 15  $\mu m$  and the 25  $\mu m$  thick guide is 0.5 and 1 mm, respectively. From microwave considerations, the electrode width cannot be reduced indiscriminantly. As the width decreases and approaches the thickness dimension, the effective phase velocity begins to change significantly because of the effect of fringing fields.

Expressions for the effective dielectric constant of microstrip structure (Ref. 10) can be used to assess the modulation efficiency which depends strongly on the degree of synchronization between the microwave and the optical wave.

Figure 11 shows the change of microwave velocity as a function of the width to thickness ratio  $W/t$  for a GaAs microstrip line. For the  $W/t$  ratio of 40, the fractional change in velocity is only about 0.025, but sufficient to bring the effective velocity of the microwave closer to those of the guided-wave modes.

The synchronous condition, therefore, appears to be easily satisfied by using the microstrip structure, which provides some room for trade-offs in mode selection and scaling of the microstrip electrode.

The effect of buffer layers on microwave propagation can be estimated from an equivalent circuit model, involving a series inductance and shunt capacitance per unit length of the transmission line, as shown in Fig. 12. This microwave

FIG. 11 EFFECT OF  $W/t$  ON VELOCITY OF PROPAGATION

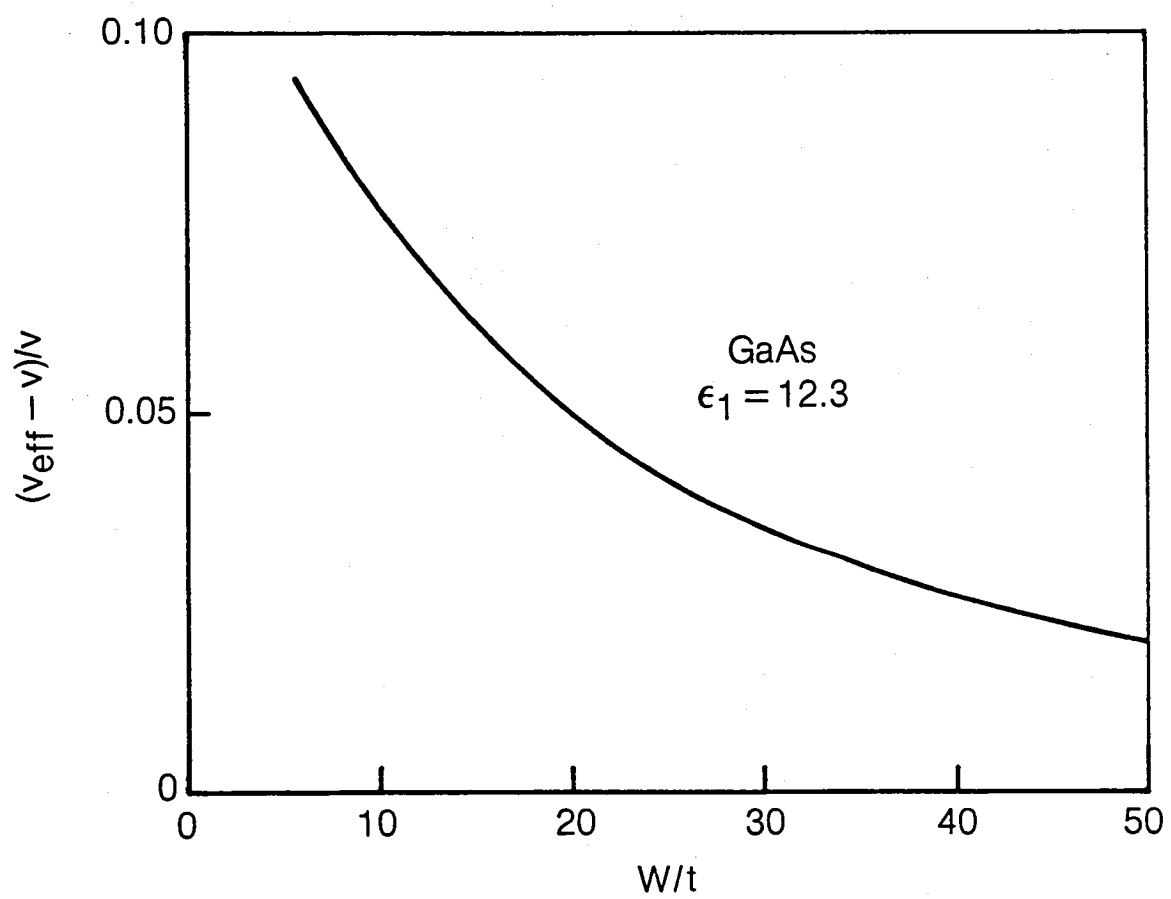
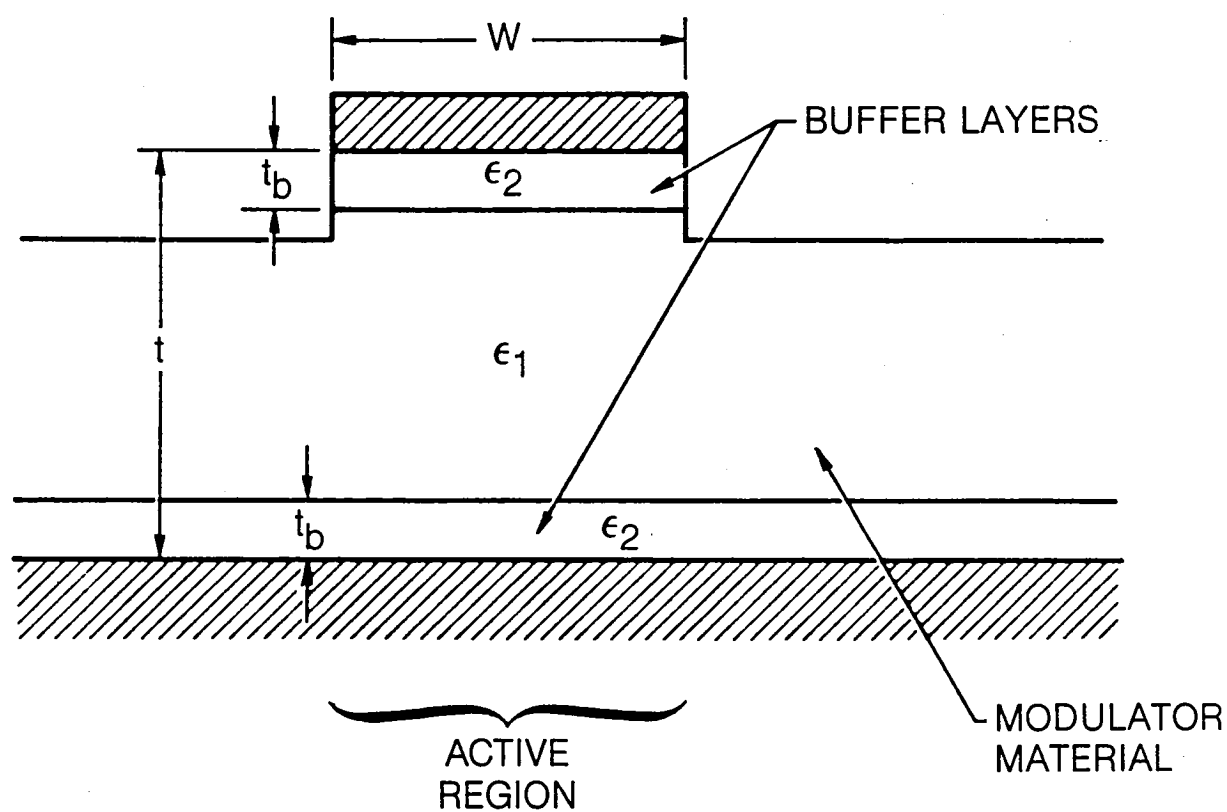




FIG. 12 CROSS-SECTIONAL VIEW OF MODULATOR WITH BUFFER LAYERS



transmission line consists mainly of a GaAs filled dielectric medium ( $\epsilon_1$ ), which is buffered from metallic electrode and ground plane by two thin layers of a lower dielectric constant ( $\epsilon_2 < \epsilon_1$ ). The width of the microstrip line is large compared to the total thickness of the dielectrics,  $t$ . The buffer layer thickness  $t_b$  is small compared to  $t$ . The velocity of propagation of this transmission line is given by

$$v = 1 / \sqrt{LC} \quad (16)$$

where  $L$  is the equivalent inductance which is essentially unchanged by introducing these buffer layers. The effective capacitance  $C$  of the transmission line can be estimated by using the following expression for the case of a uniform electric field distribution,

$$\frac{1}{C_{\text{eff}}} = \frac{1}{A} \left( \frac{t - 2t_b}{\epsilon_1} + \frac{2t_b}{\epsilon_2} \right) \quad (17)$$

The effective velocity of propagation can be expressed in terms of the velocity  $v$  in a transmission line without buffer layers as

$$v_{\text{eff}} = v \sqrt{1 + \frac{2t_b}{t} \left( \frac{\epsilon_1}{\epsilon_2} - 1 \right)} \quad (18)$$

For relatively thin buffer layers, the relative change in velocity can be approximated by the expression

$$\frac{v_{\text{eff}} - v}{v} \approx \frac{t_b}{t} \left( \frac{\epsilon_1}{\epsilon_2} - 1 \right) \quad (19)$$

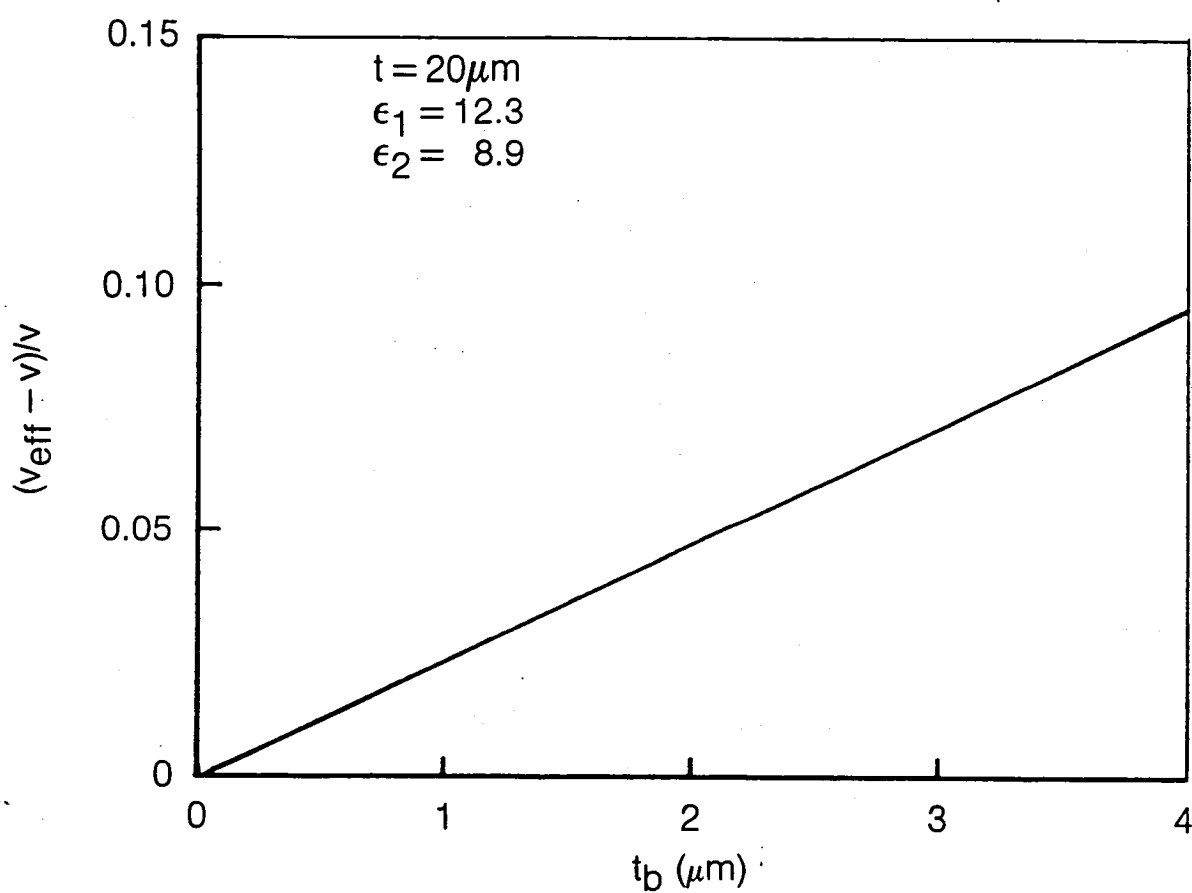
The acceptable range of values for the relative change in velocity is shown in Fig. 13, in which the  $\epsilon_1$  value was measured for bulk material at microwave frequencies, and the  $\epsilon_2$  value represents the only available measurement\* at  $f_m = 9.375$  GHz. With two  $2\text{ }\mu\text{m}$  thick buffer layers deposited onto a  $16\text{ }\mu\text{m}$  GaAs thin film, one expects a five percent increase in microwave velocity. The index of refraction  $n$  of GaAs at microwave frequencies is 3.5; for the  $10\text{ }\mu\text{m}$  guided-waves, the value  $n$  lies in the range between 3.2 and 3.3. Due to above mentioned effects, the microwave propagation in the microstrip structure is increased at a rate depending on the width of the electrode and thickness of the buffer layer and/or the composition of the waveguide. From the above analysis, it is clear that a synchronous condition between the guided IR waves and the traveling microwave can easily be achieved by properly selecting the guided mode for a modulator structural configuration.

The impedance of the main microstrip section in which electrooptic interaction between the IR and the microwave occurs is approximately  $2.7\text{ }\Omega$ . Microwave energy can be coupled efficiently into a microstrip waveguide modulator provided that several  $\lambda/4$  step impedance transformers are used to form a good match between the  $50\text{ }\Omega$  input impedance and that of the modulator. Design procedures for broadband microwave impedance transformers have been well established (Ref. 12). The impedance of the transmission line can be adjusted by varying the width of the microstrip electrode. For a thin slab of GaAs ( $25\text{ }\mu\text{m}$ ), this approach can lead to serious problems. In order to match the  $50\text{ }\Omega$  impedance, the electrode width must be reduced to below  $25\text{ }\mu\text{m}$ . At this width the line is very

---

\* Dr. James Pappis, private communication.

FIG. 13 EFFECT OF BUFFER LAYERS ON VELOCITY OF PROPAGATION



fragile and not suitable for high power operation. To overcome these problems, a thick GaAs slab (250  $\mu\text{m}$ ) has been integrated into the waveguide structure as shown in Fig. 10. With a thicker slab, a wider and more rugged electrode can be fabricated. A simplified equivalent circuit of a structure without the discontinuity is shown in Fig. 14(a). The step in the thickness causes a perturbation in the design and must be compensated by introducing additional parasitic elements, as shown in Fig. 14(b). The step discontinuity can be represented by a shunt capacitor C and the quarter-wave section which contains the discontinuity, is divided into two shorter sections with impedances of 27  $\Omega$  for the first portion and 60  $\Omega$  for the second portion. A computer model for the circuit shown in Fig. 14(b) has been established by using a measured value of 0.2 pf for the shunt capacitor. The resonant frequency for each section of the circuit over the range from 8 to 18 GHz was obtained by measuring a number of independent test samples having properly designed electrode configuration using a strong capacitance coupling technique. In this way, the large discontinuity is confined to the input and output lines, and would not affect the measured resonant frequency.

Figure 15(a) shows the entire microstrip electrode configuration with specific dimensions. Figure 15(b) gives a cross-sectional view of the transition from a conventional coaxial connector to the GaAs microstrip line. To make a good connection, the central conductor of the coax has been replaced by a pin, which is machined specially for making a planar contact with the microstrip. A special fixture, as shown in Fig. 16, is made to hold the connector in place. The calculated results for the frequency response of the modulator, which consists of both the input and the output  $3 \lambda/4$  steps impedance transformers and

FIG. 14 THE EQUIVALENT CIRCUITS FOR 3  $\lambda/4$  STEP IMPEDANCE TRANSFORMERS, (a) WITHOUT AND (b) WITH A DISCONTINUITY IN WAVEGUIDE THICKNESS

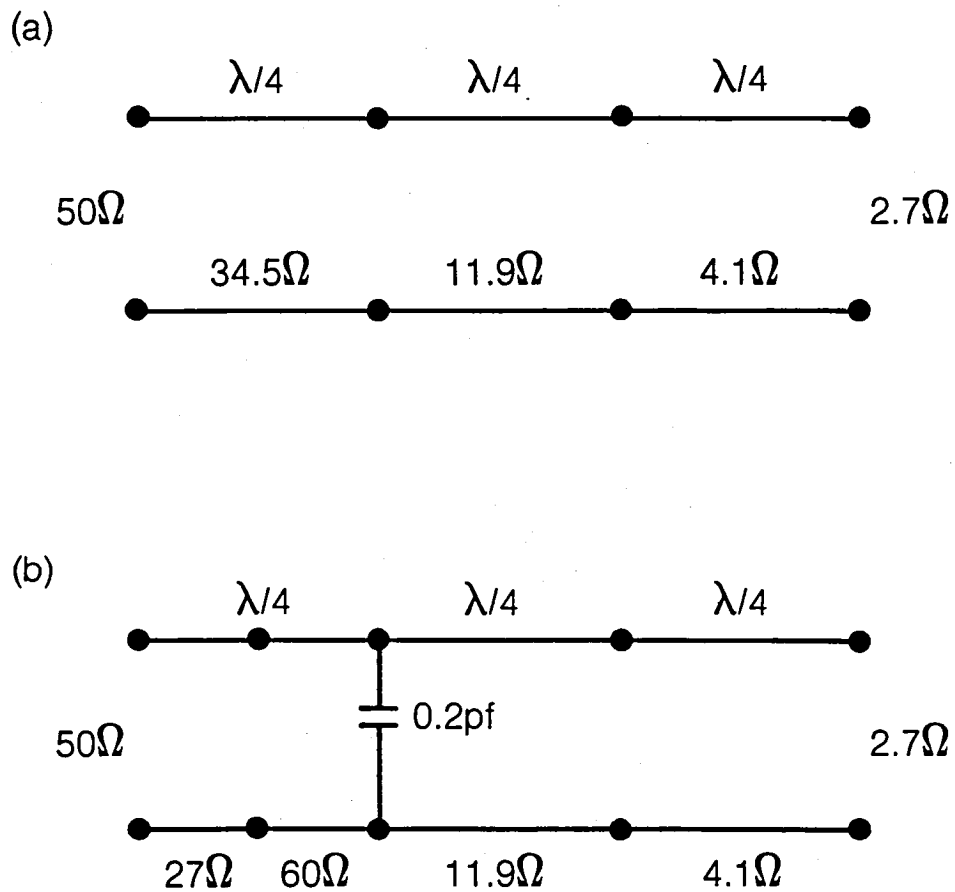


FIG. 15(a) THE GEOMETRY OF MICROSTRIP ELECTRODES INCLUDING  $3 \lambda/4$  TRANSFORMER SECTIONS

FIG. 15(b) A CROSS-SECTIONAL VIEW OF MICROWAVE INPUT OR OUTPUT TERMINAL CONNECTION

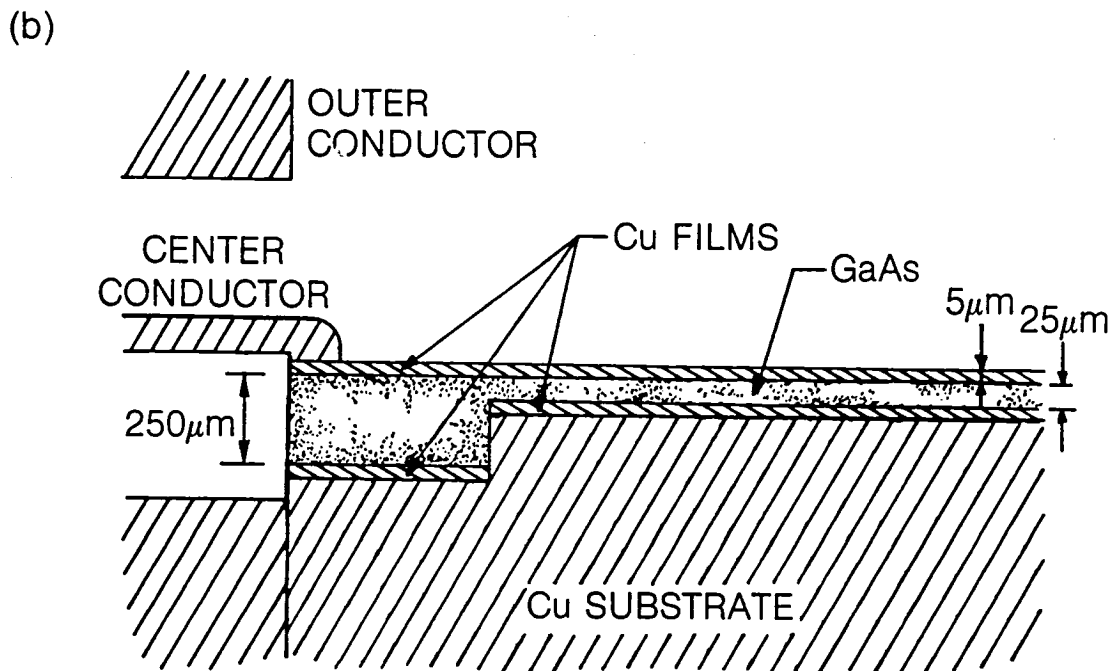
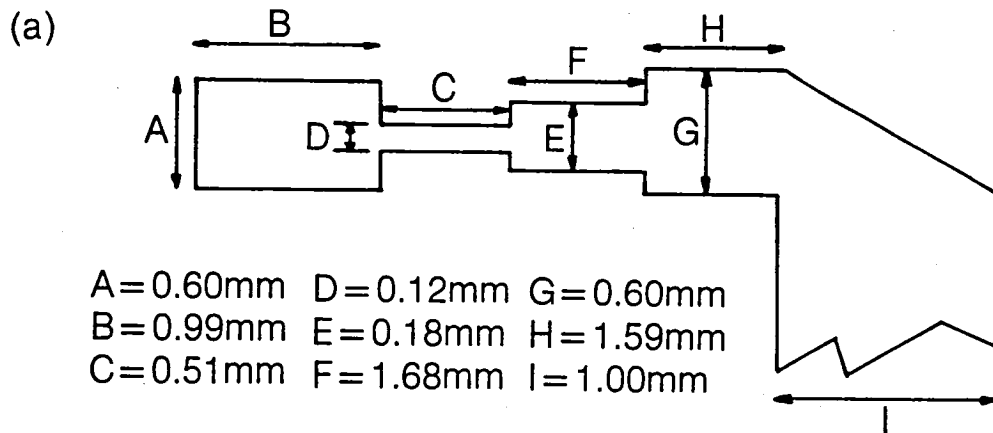
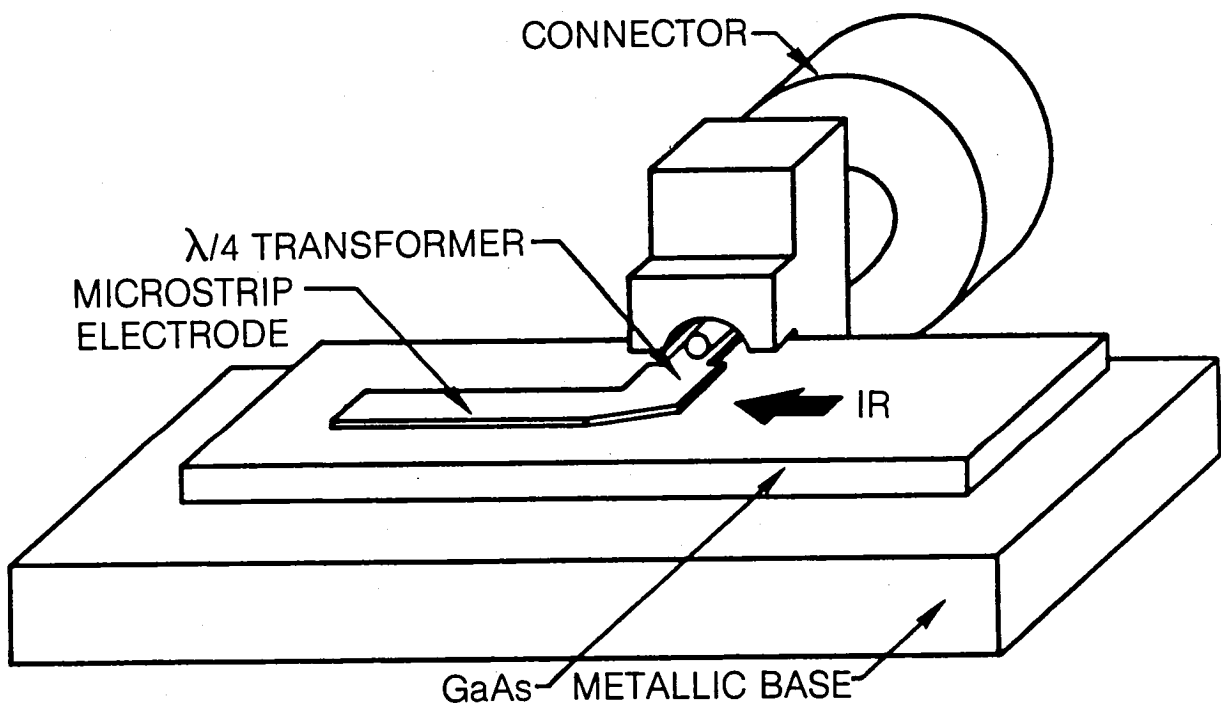


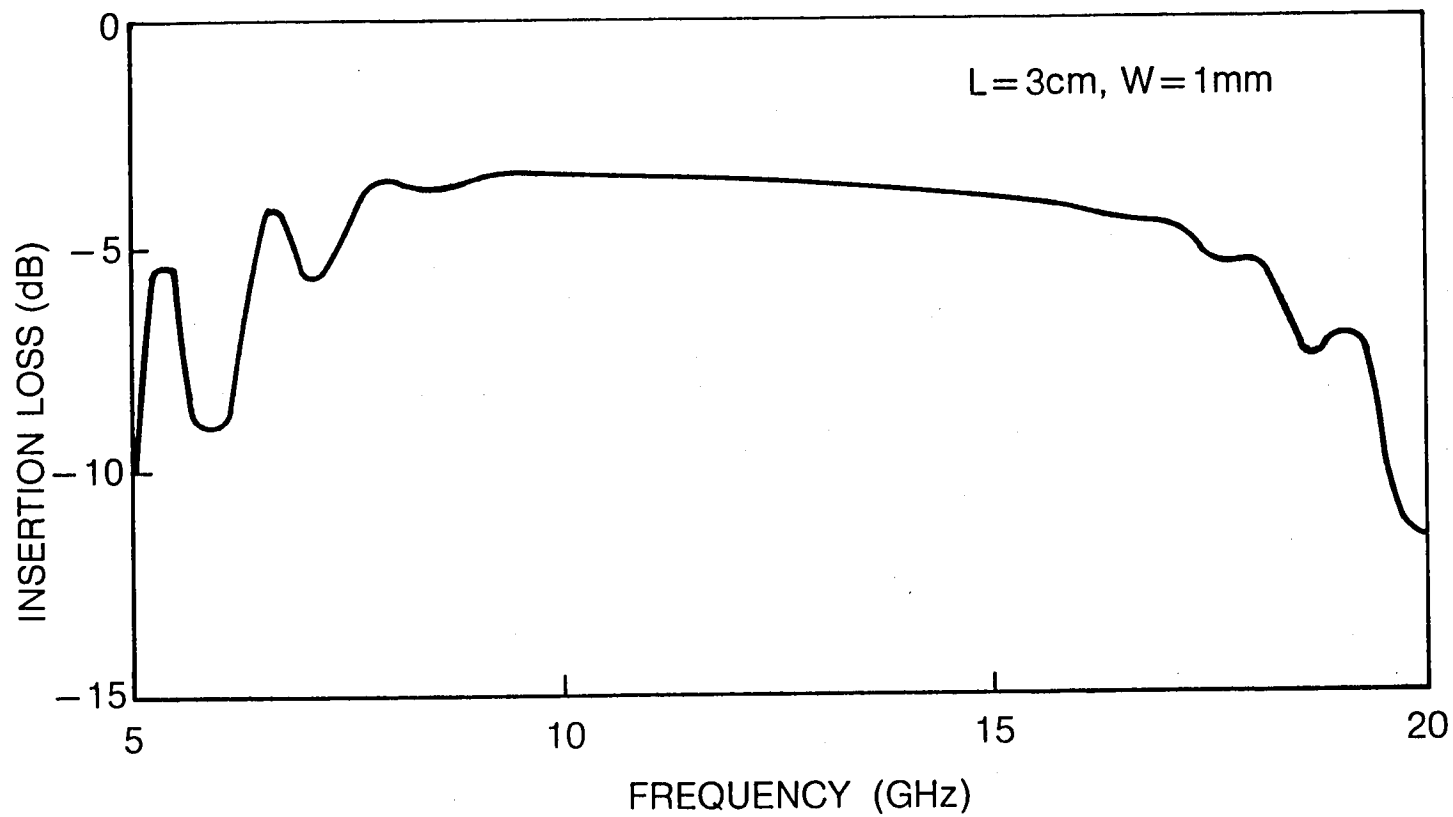
FIG. 16 THE INTERFACE BETWEEN MICROWAVE  
CONNECTOR AND WAVEGUIDE MODULATOR





3 cm long microstrip transmission line, is shown in Fig. 17. Over the frequency range varying from 8 to 18 GHz, the insertion loss is relatively flat to within 3 dB. In this calculation, the following attenuation levels associated with various sections of the microstrip transmission line were used: 0.25 dB/cm for the 50 and 60  $\Omega$  lines; 0.2 dB/cm for the 27  $\Omega$  line; 1 dB/cm for the 11.9, 4.1, and 2.7  $\Omega$  lines. The effect of 90° bends in the transmission line is not included in the calculation and turns out not to be significant. Calculated results (Fig. 17) indicate that at the ends of the useful range, a periodic variation is developed due to multiple reflections between the matching networks. Results further indicate that the choice of 10 to 1 change in thickness is an acceptable one. As the step discontinuity increases, the value for the shunt capacitance increases accordingly. This will result in an increase of the insertion loss in the upper frequency range and therefore reduce the bandwidth of the device.

FIG. 17 FREQUENCY RESPONSE OF A TRAVELING WAVE  
IR WAVEGUIDE MODULATOR



## 6.0 FABRICATION TECHNIQUES

A detailed procedure for fabricating a GaAs thin film modulator has been given previously (Ref. 5), and can be used to produce, in a routine manner, very efficient modulators for CO<sub>2</sub> lasers offering a modulation bandwidth up to 1 GHz. For producing a bandwidth greater than 1 GHz, it is necessary to modify the original procedure with a new sequence, which has been optimized by experimenting with a number of approaches. Several basic steps that are important in the fabrication procedure are:

- (1) High resistivity (Cr-doped) GaAs wafers with typical dimensions 6 cm long and 1 cm wide are lapped and polished during the initial thinning period, while maintaining a parallelism of less than 2  $\mu$ m along the entire length.
- (2) Copper blocks are used as the waveguide substrate in which channels are machined and filled with dielectric material to form the topology required for microwave impedance matching transformers.
- (3) A dicing saw is used to cut along one edge of the channel to provide the necessary interface between the microwave connector and the modulator.
- (4) A low-viscous epoxy (Epotek 353 ND) is used to bond GaAs to copper.
- (5) Ion-beam techniques are used for the final thinning of GaAs waveguide to a fixed thickness of 25  $\mu$ m and to form Cu microstrip electrodes and to channel the GaAs waveguides.

Techniques have been developed for carrying out these processing steps to obtain reliable production yield. The quality and thickness uniformity of the finished waveguide relies on the flatness of the

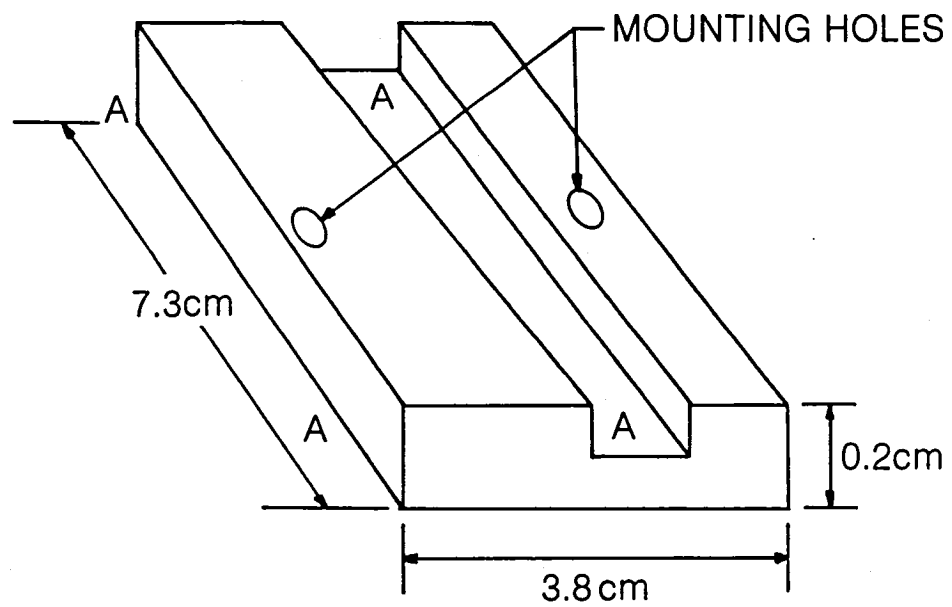
copper substrate used as the reference plane. This section describes the modified procedure necessary to achieve a good impedance matching in order to obtain a flat frequency response over a 30 GHz range.

A large supply of waveguide substrates is prepared by machining copper blocks (7.3 cm x 3.8 cm x 2 mm) as shown in Fig. 18(a), with channel dimensions 0.95 cm wide and 0.3 mm deep. A Cu block with an optically polished surface is bonded to a flat steel block. The steel block is attached to the copper block by means of two screws through the mounting holes. The screws force one of the copper block surfaces flatly against the steel block until the wax sets. The steel block is then bolted to an optical polishing fixture manufactured by Logitech (PP5). Before attaching to the optical polishing fixture, a GaAs wafer (6 cm long, 4 mm wide and 0.5 mm thick) is bonded to the copper block, as shown in Fig. 18(b). The bonding substance is a thin layer (1 to 2  $\mu\text{m}$ ) of Epotek 353 ND, manufactured by Epoxy Technology Corporation. The bonded surface of this GaAs wafer has been ion-beam plated with a 5  $\mu\text{m}$  thick copper film. This piece of GaAs filler constitutes a part of the impedance transformer network.

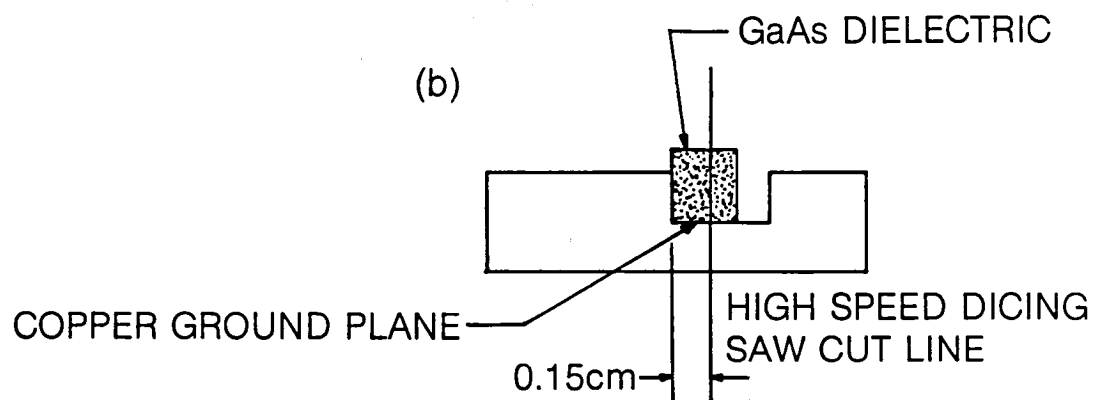
The entire assembly as described above is attached to a polishing fixture, which has an outer ring and inner mounting area for lapping and polishing. The outer ring acts as a guide on the lapping plate. The inner portion of the polishing fixture is free to move in the vertical direction with respect to the outer ring. During lapping, the surface of the dielectric filler is examined repeatedly by placing the polishing fixture on an X-Y table supported by three micrometers at three points separated by  $120^\circ$  along a circle. The parallelism of

FIG. 18 CHANNELED Cu SUBSTRATE FOR GaAs FILTER

(a)



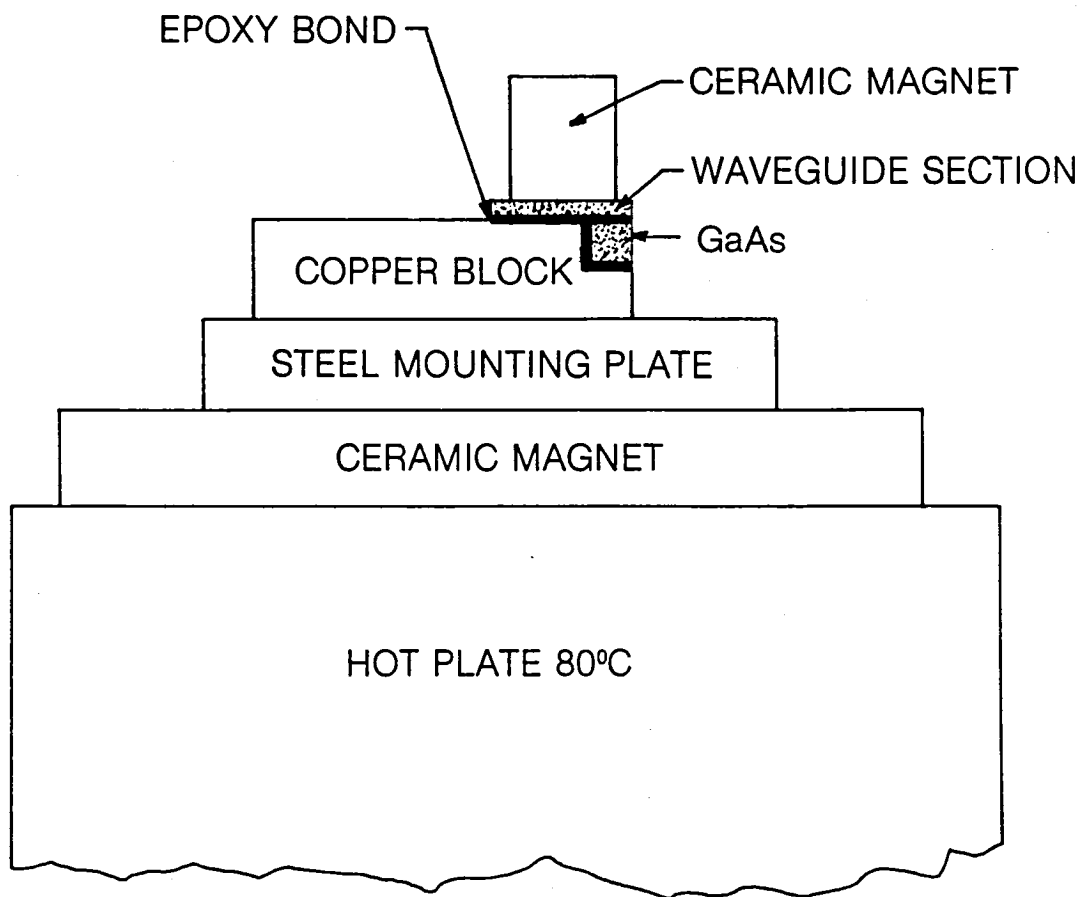
(b)



the lapped surface is monitored by using a non-contacting air-bearing hover probe. Any wedging in the wafer can be corrected by balancing the outer ring of the polishing fixture with these three micrometers. The surface of the outer ring must be adjusted parallel to the surface of the copper block by using the adjusting screws on the polishing fixture. The dielectric filler is lapped down to a thickness of 0.23 mm with a 27 micron grit in the lapping machine, which is also manufactured by Logitech (PM-2). At this point, the lapped surface of GaAs filler is co-planar with the surface of the copper block. A high speed dicing saw is used to section the copper block along the line as shown in Fig. 18(b) to provide a proper width of the dielectric filler (1.52 mm), which forms the necessary step discontinuity in the microwave transmission line.

Prior to bonding the upper GaAs waveguide section, the copper block is cleaned ultrasonically to remove any grit residue from the surface. A GaAs wafer, having a copper ground plane ion-beam plated on one of its surfaces, is bonded to the dielectrically filled copper block. In the area where the waveguide overlaps the dielectric filler, it does not have the copper film. Figure 19 depicts the method by which the GaAs wafer is epoxy bonded to the block using magnets to insure a flat and uniform bonding layer having a typical thickness of 1 to 2  $\mu\text{m}$ . After curing the epoxy, the device is remounted to the polishing fixture. The outer ring is first referenced parallel to the hover probe as described before. The surface of the Cu block is then adjusted to be parallel to the outer ring of the polishing fixture. The waveguide section is lapped to a thickness of 150  $\mu\text{m}$  using a 3 micron grit size aluminum oxide slurry on a glass plate inserted into the PM-2 lapping machine.

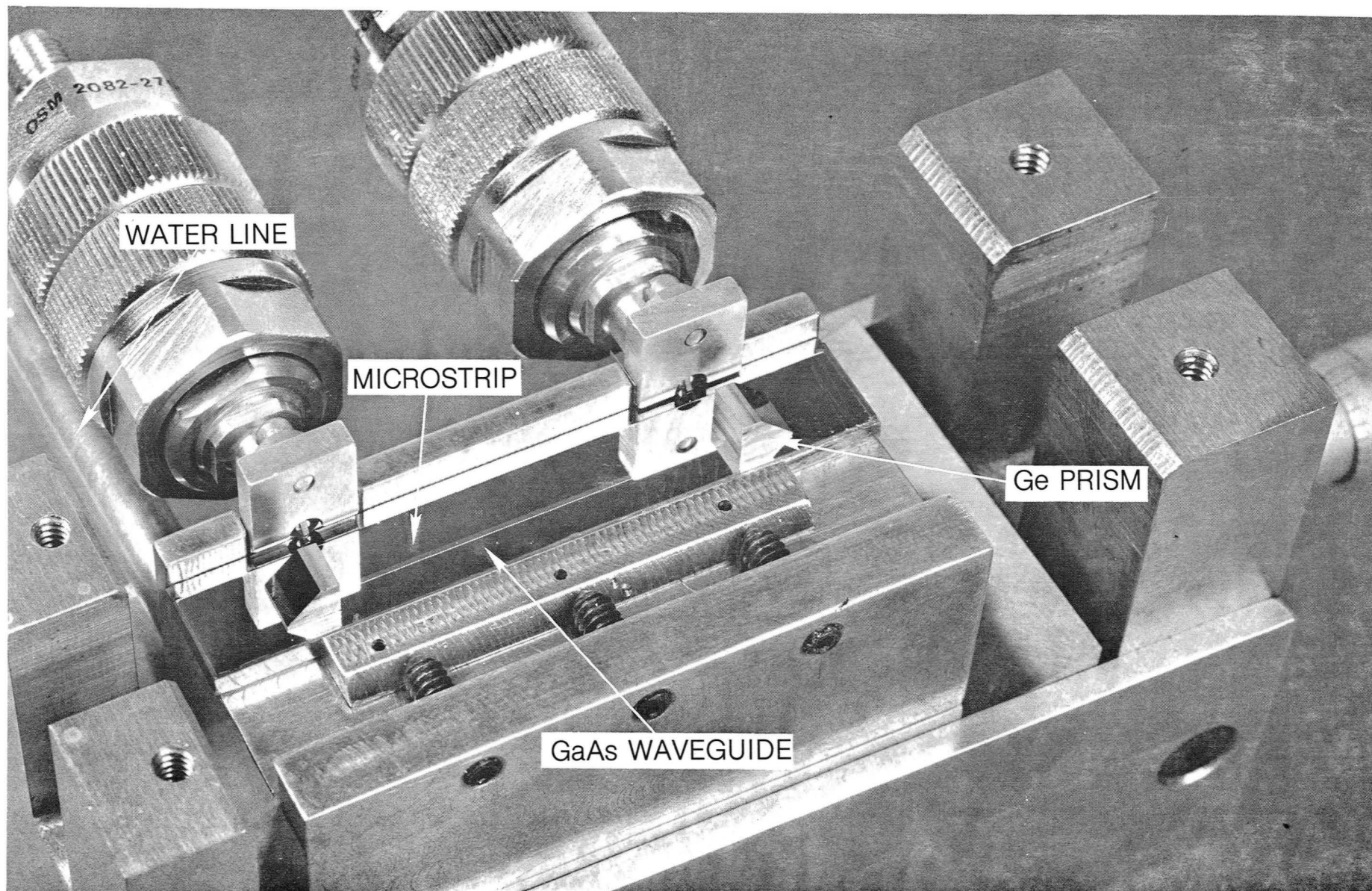
FIG. 19 A METHOD FOR BONDING GaAs WAFERS TO Cu



The steel block is then removed from the polishing fixture. The thickness of the waveguide is measured at three points along its length using an IR spectrophotometer (Nicolet MX-2) in the reflectance mode with a 0.5 mm aperture. A series of fringe-like patterns resulting from interference between the reflections from the upper and the lower surfaces is obtained and can be used to calculate the thickness as well as the variation in thickness. Once the thickness variation is determined, the waveguide is remounted to the polishing fixture. By iteration, any wedging in the waveguide can be corrected. This compensation process may be repeated several times before polishing down to a thickness of about 75  $\mu\text{m}$ . At this point, the waveguide thickness is uniform to within 1  $\mu\text{m}$ . The waveguide is subject to chemo-mechanical polishing by using a Buehler Chemomet polishing pad in a diluted solution of sodium hypochlorite mixed with distilled water in 1:10 ratio. The final thinning of the waveguide from 50  $\mu\text{m}$  to 25  $\mu\text{m}$  is accomplished by using an ion-beam milling machine. Figure 20 shows a typical waveguide modulator assembled in a housing with the top plate removed. The copper substrate is bolted onto a water-cooled copper base plate, which has two slots for positioning the interface fixtures for microwave connectors. Also shown in this figure are two Ge prisms located at the two bends of a microstrip transmission line.



FIG. 20 AN IR WAVEGUIDE MODULATOR INTEGRATED  
WITH A TRAVELING-WAVE MICROSTRIP TRANSMISSION LINE





## 7.0 RESULTS AND DISCUSSION

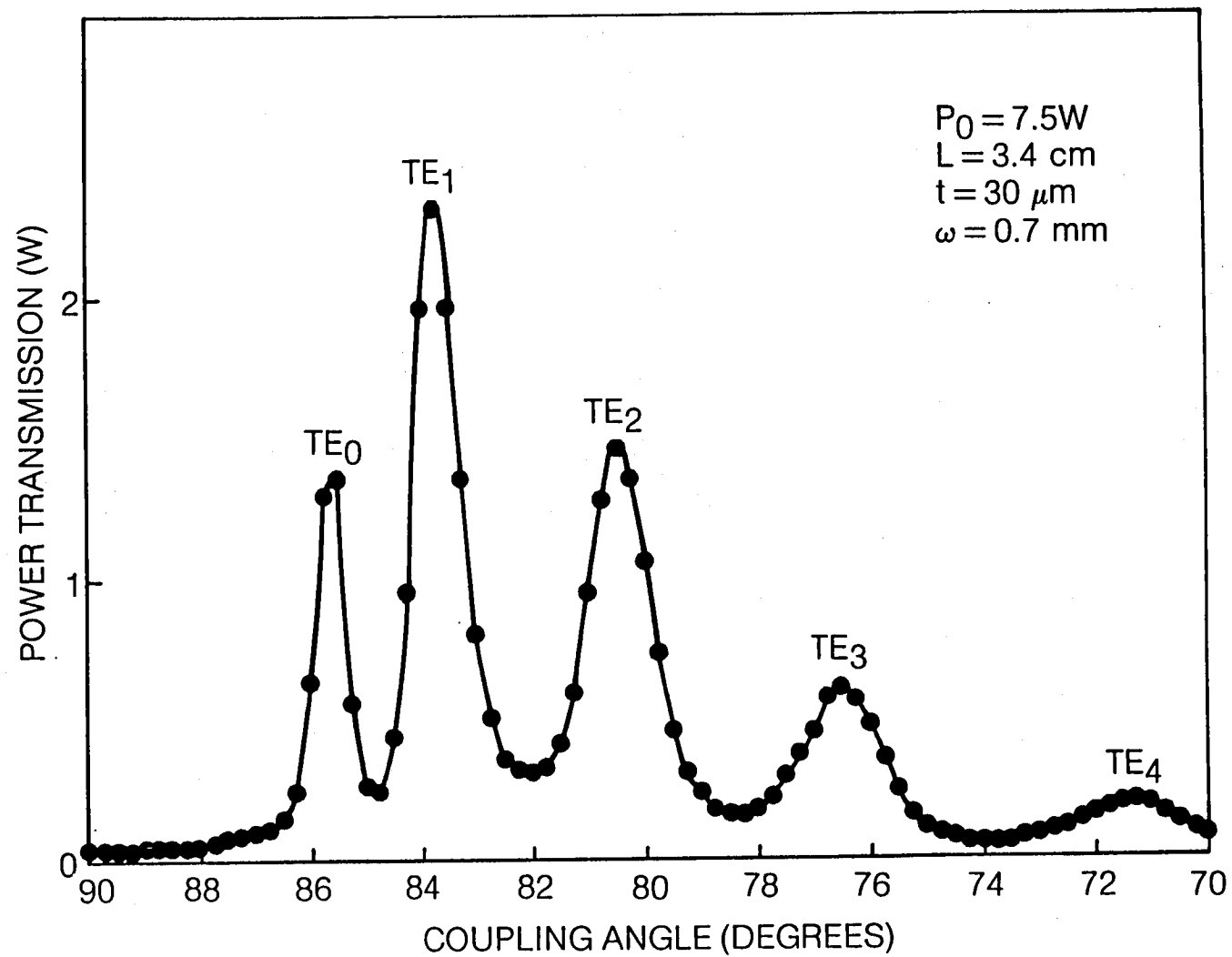
The output of this tunable IR source depends on several parameters, including the power levels of the CO<sub>2</sub> laser P<sub>O</sub>, and the microwave P<sub>m</sub>, the transmission characteristics and frequency response of the waveguide modulator, the Fabry-Perot filter and the White cell. With the exception of the waveguide modulator, all components of the system are commercially available and provide very reliable performance over a wide range of operating conditions. For this reason, the measured system performance has been normalized with respect to fixed optical and microwave power. Special emphasis is given to one of the most reliable modulator structures having a single dielectric layer, for which most of the experimental results are obtained. A procedure has also been developed for making the multilayered structure, however, experimental results are inadequate to establish a representative data base for this device.

The output of the tunable source in terms of its sideband power P<sub>s</sub> is proportional to the produce of P<sub>O</sub> and P<sub>m</sub>:

$$P_s = \eta P_O P_m \quad (20)$$

where  $\eta$  is the power conversion efficiency of the system. At a fixed microwave power input,  $\eta$  is simply a power conversion ratio of P<sub>s</sub>/P<sub>O</sub>, as determined by Eq. (16), where P<sub>O</sub> is the carrier power transmitted through the waveguide. For a typical 25  $\mu$ m thick GaAs waveguide modulator, optical transmission of various guided-wave modes thorough 3.5 cm long microstrip electrodes is shown in Fig. 21.

FIG. 21 POWER TRANSMISSION OF GUIDED-WAVE MODE FROM A TYPICAL WAVEGUIDE MODULATOR



Results are obtained by using germanium right angle prisms as the input-output couplers. As predicted, the highest transmission is obtainable from the  $TE_1$  mode, at values varying from 25 to 36 percent, depending on the quality of the guide. Because of the narrow channel width (1 mm), the  $TE_0$  mode cannot be excited efficiently by these couplers. The transmission loss of the  $TE_1$  mode is mainly caused by the absorption of electrodes. As discussed previously, this situation can be improved by using the MLWG structure.

Figure 22 is an oscilloscope trace of the sidebands and the carrier waveforms. These spectral outputs are obtained by applying a saw-tooth voltage (0 to 1000 v) from a ramp generator to the piezoelectric transducers PZTs, which sweep the Fabry-Perot mirror spacing by one free spectral range ( $\sim 50$  GHz). A slight non-linear response in PZTs causes the asymmetric display of the sidebands. By passing the modulated output through a multipath White cell filled with  $CO_2$  gas at a pressure of 35 Torr and a temperature of  $60^\circ C$ , the ratio of the sideband to the carrier power of the P(18) line increases by a factor of 30 dB as shown in Fig. 23. At a constant microwave input power of 10 W, a power conversion of about 0.5 percent from the carrier to one single sideband can be obtained over a frequency range from 8 to 18 GHz. Figure 24 shows the measured sideband response over only the Ku band. Experimentally, it has been shown that  $P_s$  increases linearly with increasing  $P_m$  values up to 80 W. Similar results (not shown in Fig. 24) have also been obtained in the X band. Figure 25 shows the frequency response measurements of a typical waveguide modulator using a microwave 2-22 GHz signal generator (HP83590A) and a network analyzer (HP8410A). The top trace is the reference level obtained for a straight-through signal without the modulator.

## FIG. 22 OUTPUT SPECTRUM ANALYZED BY A FP FILTER

VERTICAL SCALE =  $50\mu\text{V/cm}$

HORIZONTAL SCALE IS NON-LINEAR AND A CHARACTERISTIC OF THE PZT FOR TUNING OF THE FILTER

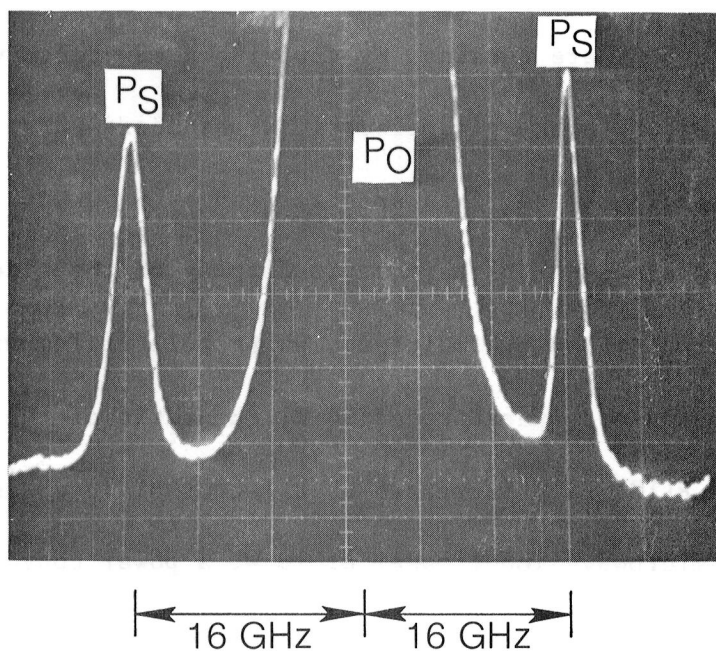


FIG. 23 OUTPUT SPECTRUM THROUGH A WHITE CELL  
( $T = 60^{\circ}\text{C}$ ,  $P = 35\text{Torr}$ )

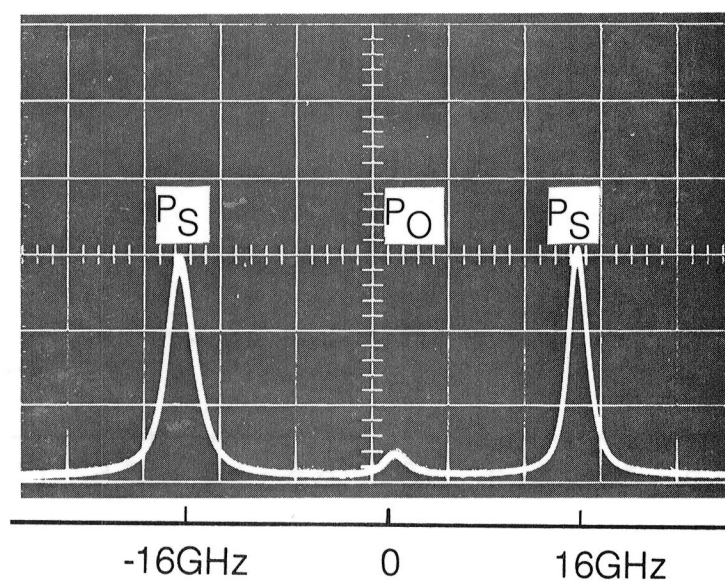


FIG. 24 MEASURED SIDEBAND POWER IN THE Ku BAND

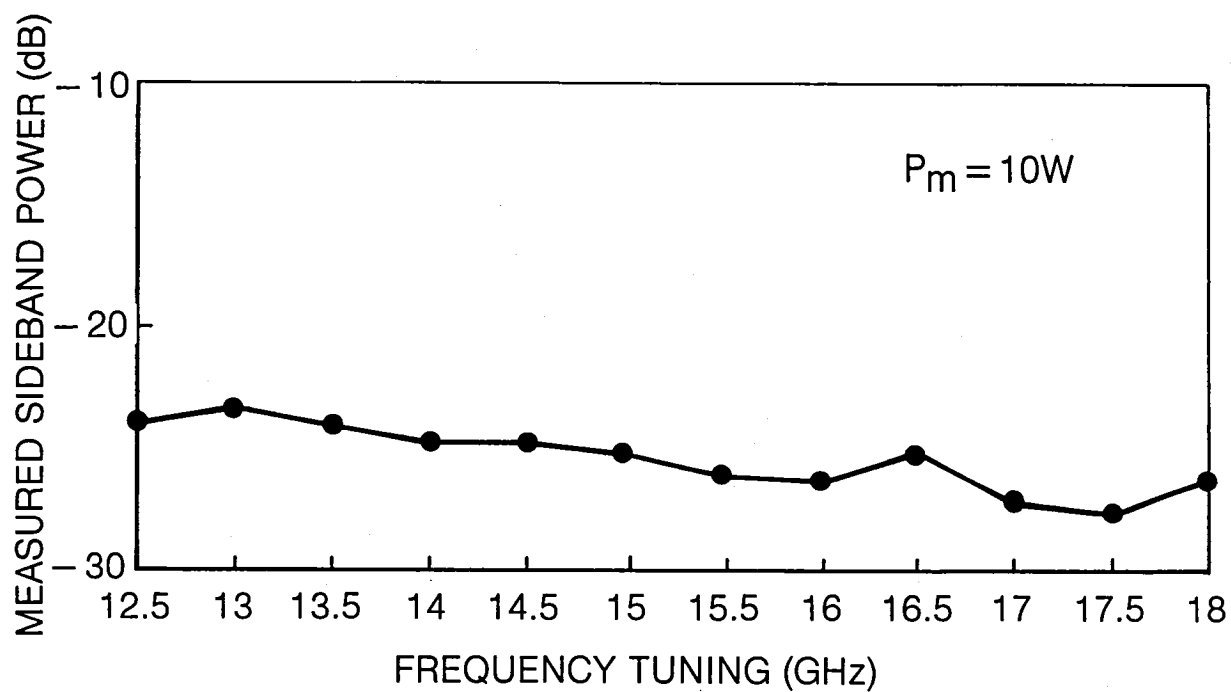
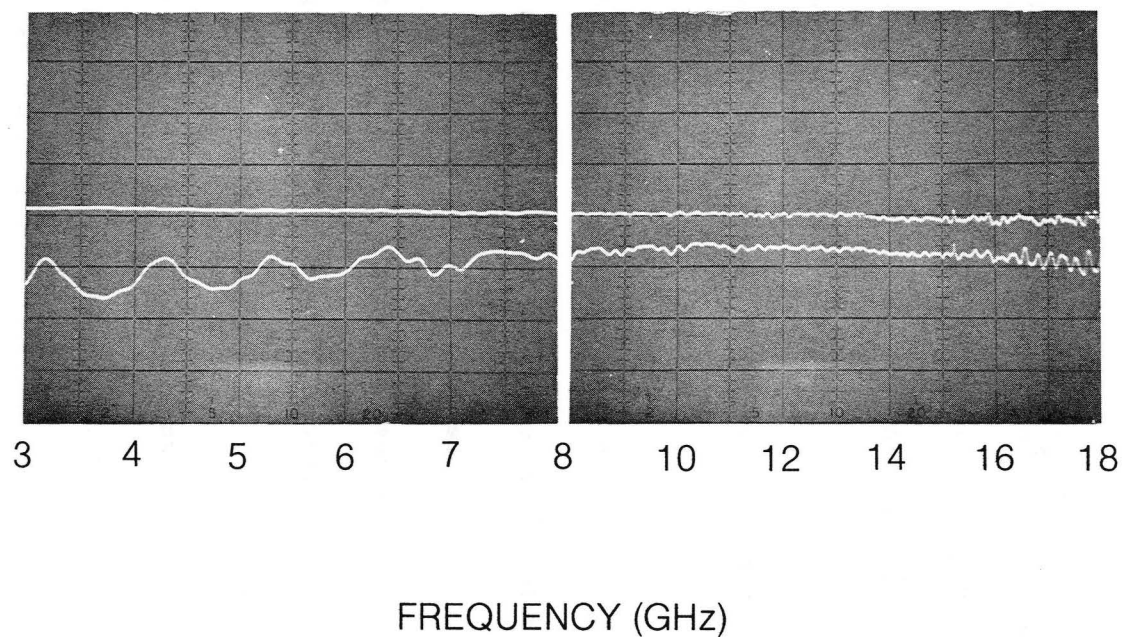




FIG. 25 MICROWAVE TRANSMISSION MEASUREMENTS. TOP TRACE IS A REFERENCE LEVEL WITHOUT MODULATOR (VERTICAL SCALE: 10 dB/cm). LOWER TRACE IS THE INSERTION LOSS OF A TYPICAL GaAs WAVEGUIDE MODULATOR



The lower trace represents the insertion loss when a modulator is inserted into the circuit. Results indicate that the frequency response of this modulator is flat to within 7 dB over a frequency range varied from 3 GHz to 18 GHz, and to within 3 dB over 8 to 18 GHz, consistent with the calculated results based on a computer model using measured values for various sections of the designed microstrip line. At  $P_m=30$  W and  $P_o=20$  W, approximately 1.5 percent of the transmitted carrier power ( $\sim 6-7$  W) can be converted into the sideband. This corresponds to a tunable IR laser output of  $\sim 100$  mW. The prospect for increasing this value by a factor of five is not unrealistic, and can be reached by increasing the input power levels and by using an improved MLWG modulator structure.

The availability of this compact tunable source which can provide a moderate but inherently stable output should fulfill the requirement for numerous field applications, including remote sensing of the earth, planetary and stellar atmospheres, combustion process controls and environmental protection, injection locking of TEA laser amplifiers, ultra-high resolution spectroscopy, isotope separation, and frequency-multiplex communication.

The author wishes to acknowledge the contributions of M. Gilden for designing microwave circuitry, R. Wagner for fabricating the modulators, and G. Sachse for many helpful discussions. He also wishes to thank G. Carrier for his technical assistance.

## 8.0 REFERENCES

1. Cheo, P. K.: Generation and Applications of 16 GHz Tunable Sidebands from a CO<sub>2</sub> Laser. Laser Spectroscopy III, Ed. by J. L. Hall and J. L. Carlsten, Springer Verlag, Berlin Heidelberg, New York, pp. 394-401, (1977).
2. Cheo, P. K. and M. Gilden: Continuous Tuning of 12 GHz in Two Sidebands of CO<sub>2</sub> Laser Lines. Opt. Lett., 1, pp. 38-39, (1977).
3. Sachse, G.: Microwave Tunable Laser Source: A Stable, Precision Tunable Heterodyne Local Oscillator, Proc. Heterodyne Systems and Technology Conf., Williamsburg, VA, March 25-27 (1980).
4. Cheo, P. K.: CO<sub>2</sub> Lasers. Advances in Lasers, Ed. by A. Levine and A. DeMaria, Marcel Dekker Publishing Co., pp. 111-262, (1971).
5. Freed, C.: Absolute Frequency Calibration of the CO<sub>2</sub> Isotope Laser Transitions. Conference Precision Elect. Measurements, June 28-July 1, Boulder, CO (1976).
6. Butler, J. F., and T. C. Harmans: Long-Wavelength Infrared PbSnTe Diode Lasers. Appl. Phys. Lett. 12, pp. 347-349, (1968).
7. Carter, G. M.: Tunable High-Efficiency Microwave Frequency Shifting of Infrared Lasers. Appl. Phys. Lett. 32, pp. 810-812, (1978).
8. Cheo, P. K. and R. Wagner: Infrared Electrooptic Waveguides. IEEE J. Quant. Elect. QE-13, pp. 159-164 (1977).
9. Chang, W. S. C. and K. W. Loh: Theoretical Design of Guided Wave Structure for Electrooptical Modulation at 10.6  $\mu$ m. IEEE J. Quant. Elect., QE-8, pp. 463-470 (1972).

#### REFERENCES (Concluded)

10. Ulrich, R.: Theory of Prism-Film Coupler by Plane Wave Analysis. J. Opt. Soc. Amer. 60, pp. 1337-1350, (1970).
11. Gupta, K. C., R. Garg, and I. J. Bahl: Microstrip Lines and Slot-Lines. Artech House, Inc. (1979).
12. Young, L.: Tables for Cascaded Homogeneous Quarter-Wave Transformers. IRE Trans. MTT-7, 233 (1959).

1. Report No. NASA CR-172479		2. Government Accession No.		3. Recipient's Catalog No.	
4. Title and Subtitle ADVANCED INFRARED LASER MODULATOR DEVELOPMENT				5. Report Date December 1984	
				6. Performing Organization Code	
7. Author(s) P. K. Cheo, R. Wagner and M. Gilden				8. Performing Organization Report No. R83-925985-6	
9. Performing Organization Name and Address United Technologies Research Center East Hartford, Connecticut 06108				10. Work Unit No.	
				11. Contract or Grant No. NAS1-16904	
12. Sponsoring Agency Name and Address National Aeronautics and Space Administration Langley Research Center, Hampton, Virginia 23665				13. Type of Report and Period Covered Contract Report	
				14. Sponsoring Agency Code	
15. Supplementary Notes Technical Monitor: Glen Sachse Final Technical Report					
16. Abstract  A parametric study was conducted to develop an electrooptic waveguide modulator for generating continuous tunable sideband power from an infrared CO <sub>2</sub> laser. Parameters included were the waveguide configurations, microstrip dimensions device impedance, and effective dielectric constants. An optimum infrared laser modulator was established and has been fabricated. This modulator represents the state-of-the-art integrated optical device, which has a three-dimensional topology to accommodate three $\lambda/4$ step transformers for microwave impedance matching at both the input and the output terminals. A flat frequency response of the device over 20 HGz ( $\leq 3$ dB) has been achieved. Maximum single sideband to carrier power greater than 1.2% for 20 W microwave input power at optical carrier wavelength of 10.6 $\mu\text{m}$ has been obtained.					
17. Key Words (Suggested by Author(s)) Integrated Optics, Tunable IR Sources, Traveling-wave E-O Modulators				18. Distribution Statement  Unclassified	
19. Security Classif. (of this report) Unclassified		20. Security Classif. (of this page) Unclassified		21. No. of Pages	
				22. Price	





